Doctoral Dissertations   Student Theses and Dissertations

1972

The eikonal distorted wave Born approximation for the excitation of hydrogen by impact with hydrogen and helium in the intermediate energy range

Richard Homer Shields

Recommended Citation

THE EIKONAL DISTORTED WAVE BORN APPROXIMATION

FOR THE EXCITATION OF HYDROGEN BY IMPACT

WITH HYDROGEN AND HELIUM IN THE INTERMEDIATE ENERGY RANGE

by

RICHARD HOMER SHIELDS, 1945-

A DISSERTATION

Presented to the Faculty of the Graduate School of the

UNIVERSITY OF MISSOURI-ROLLA

In Partial Fulfillment of the Requirements for the Degree

DOCTOR OF PHILOSOPHY

in

PHYSICS

1972

Jerry L. Peacher
Advisor

Adawi'

John T. Park

Y W Sund

A. J. Bevier

ABSTRACT

An eikonal approximation is applied to atom-atom scattering in the intermediate energy range. The theory and the form of the eikonal approximation are reviewed. Also a brief survey of previous theoretical methods for all energy ranges is included.

In particular, the differential and total cross sections for the excitation of hydrogen to the 2s and 2p states by impact on hydrogen and helium atoms have been calculated using the eikonal distorted wave Born approximation (DWBA) for the incident energy range of 2.25-100 keV. The eikonal DWBA differential cross sections are compared to the differential cross sections given by the first Born approximation. The eikonal DWBA results predict a lower cross section for smaller angles and a much slower fall off with larger angles than the first Born approximation. For H-He scattering at 10 keV, the eikonal DWBA differential cross section is compared to experimental data. It was found to agree quite well in shape and slope but differed in magnitude by a factor of four.

The eikonal DWBA total cross sections were compared to other theoretical calculations and were found to follow closely to the multistate impact parameter calculations. In the limit of high energies and very small angle scattering, the results for the eikonal DWBA total cross section were shown to reduce to the 2-state distortion approximation.

Also for H-He scattering, a comparison of total cross sections is made between the eikonal DWBA results and experimental data. Agreement

is found to be poor at the lower energies where the eikonal DWBA
results are not expected to be valid and good at the higher energies.

ACKNOWLEDGEMENTS

I would like to acknowledge the cooperation from my advisor, Dr. Jerry L. Peacher. His initial suggestions started the author on this work and his continuing advice and cooperation enabled the work to be completed successfully.

I would also like to thank the Faculty of the Physics Department for their many contributions and support. I would like to thank the Physics Department for the National Defense Education Act Fellowship and for other financial support.

I, emphatically, wish to thank my wife, Barbara Shields. Her constant support and her unfailing belief in me truly made this work possible.

TABLE OF CONTENTS

Table of Contents (continued)

LIST OF ILLUSTRATIONS

List of Illustrations (continued)

List of Illustrations (continued)

I. INTRODUCTION

There has been a considerable amount of interest in the theoretical and experimental study of atom-atom collisions. A great deal of this study has been centered on the collisions of hydrogen atoms with hydrogen and helium atoms. These systems are simple enough that they lend themselves to theoretical calculations, but yet sufficiently complex to give rise to the main types of inelastic transitions observed.

The first theoretical paper on the subject was by Bates and Griffing[1] in 1953. They studied H-H collisions using the Born approximation in the high energy range. Moisewitsch and Stewart[2] in 1954 performed a similar calculation for H-He collisions.

The interest in the subject seemed to lag at this point and was not renewed until the first experimental results were published. In 1967 at the Fifth International Conference on the Physics of Electronic and Atomic Collisions, Ankudinov, Andreev, and Orbeli[3] presented the experimental cross sections for the processes

$$H(1s) + He(1^1S) \rightarrow H(2s, 2p_0, 2p_\pm) + He(1^1S) \qquad (1.1)$$
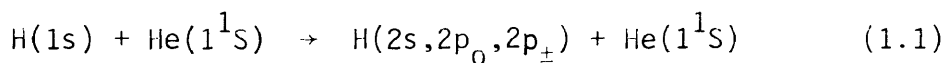
for the energy range of 0-40 keV. These results were later published by Orbeli, Andreev, Ankudinov, and Dukelskii.[4] The 2p excitation cross sections were also measured by Dose, Gunz, and Meyer.[5] Their results were slightly lower.

With the advent of the computer, complicated theoretical calculations became feasible to do. The multistate impact parameter

method which requires the numerical solution of a set of coupled differential equations was applied to the processes

$$H(1s) + H(1s) \rightarrow H(2s, 2p_0, 2p_\pm) + H(1s) \qquad (1.2)$$
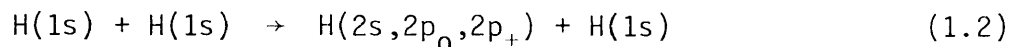
by Flannery[6] in the intermediate energy range.[7] Then the method was applied to H-He collisions, Eq. (1.1), in a paper by Flannery[8] and in another paper by Levy[9]. The 2s excitation cross sections agreed well with the experiment of Orbeli, et al.[4] However, the 2p excitation cross section shows a large discrepancy between the theory of Flannery[8] or Levy[9] and the experiments of Orbeli, et al.[4] and Dose, et al.[5] Even the first Born approximation shows better agreement with the experimental results. Levy[9] has pointed out that the difference may be due to the neglect of electron exchange and cascade effects.

Recently there have been more experiments on the H-He collision, Eq. (1.1), over a wide energy range. Birely and McNeal[10] have measured the total cross sections as a function of energy in the range of 1-25 keV. Hughes and Song-Sik Choe[11] have done the experiment for an energy range of 20-125 keV. The latest experiment is by Sauers, Nichols, and Thomas.[12] They measured the differential cross sections for the 2s excitation of hydrogen for an incident energy of 5-25 keV.

The interest in atom-atom collisions stems from a desire to understand the complicated processes that occur in the upper atmosphere. The discovery of the Doppler-shifted hydrogen lines in the auroral spectrum gave direct evidence that excitations of energetic

particles are important in interpreting the aurora. Measurements have been made of the flux and the energy spectrum of protons in the upper atmosphere. Large fluxes of protons were found in the intermediate energy range of 1-10 keV. Consequently, a large flux of hydrogen atoms would be present from charge transfer processes. The role of energetic protons and hydrogen atoms in the upper atmosphere has been the source of extensive study and much speculation.[13] The basic understanding of such processes as Eqs. (1.1) and (1.2) can lead to a long range understanding of complicated atmospheric phenomena.

In this paper I apply a new method to the processes mentioned in Eqs. (1.1) and (1.2). This new method is the eikonal distorted wave Born approximation (DWBA) and was first proposed by Chen, Joachain, and Watson[14] for electron-atom scattering in the intermediate energy range.

The basic feature of this method is a correction factor to the total wave function used in the Born approximation. This factor allows for the distortion of the incoming and outgoing wave functions as the multistate impact parameter method does. However, differential cross sections are obtained from the eikonal DWBA while the multistate impact parameter method yields only total cross sections.

In section II a review of the theoretical methods used in atom-atom collisions will be given. The theory of the eikonal DWBA will be presented in section III, while the results for the H-H collisions, Eq. (1.2), and the H-He collisions, Eq. (1.1), will be given in sections IV and V, respectively. The conclusion is presented in

section VI along with a discussion of the problems and the future of the eikonal DWBA.

II. REVIEW OF THE LITERATURE

A. Low Energy

At present there is no direct method available for the entire
energy range for the collisions of atoms. Approximations have been
developed that are valid for low energy collisions and others for
high energy collisions. At low energy where the formation of a
quasimolecule during the collision has a high probability, the
perturbed stationary state (PSS) method is used.[15-18]

This method adopts a procedure similar to the Born-Oppenheimer
approximation for diatomic molecules. The adiabatic assumption that
is made asserts that the electrons follow the nuclear motion without
making any transitions from one electronic state to another, but
rather the electronic wave function itself is deformed slowly by the
nuclear motion. The mathematical consequence of this hypothesis is
that the wave function is separable into a product of two functions,
one describing the electronic motion and the other the nuclear
motion.

Consider two atoms of masses M_A and M_B separated by an inter-
nuclear distance $\vec{R}$. The notation $\vec{r}_A$ and $\vec{r}_B$ represents the positions
of the electrons of atom A and B, respectively. Following the Born-
Oppenheimer approximation, we neglect the mass of the electron in
comparison to the mass of the nucleus. The approximate wave equation
in the center of mass coordinate system in atomic units[19] is

$$[- \frac{1}{2M} \nabla^2_{\vec{R}} - \frac{1}{2} \nabla^2_{\vec{r}_A} - \frac{1}{2} \nabla^2_{\vec{r}_B} + V_A(\vec{r}_A) + V_B(\vec{r}_B) + V_I(\vec{r}_A,\vec{r}_B,\vec{R}) + U(\vec{R})]$$

$$x \ \Psi(\vec{r}_A,\vec{r}_B,\vec{R}) = E\Psi(\vec{r}_A,\vec{r}_B,\vec{R}) \tag{2.1}$$

where M is the reduced mass,

$$M = M_A M_B / (M_A + M_B) \tag{2.2}$$

and E is the total energy of the system. V_A and V_B are the internal atomic potentials of atoms A and B, respectively; V_I is the electronic interaction potential between atoms A and B; and U is the nuclear coulomb interaction potential between atoms A and B.

For a fixed nuclear separation, the electronic wave equation is

$$[- \frac{1}{2} \nabla^2_{\vec{r}_A} - \frac{1}{2} \nabla^2_{\vec{r}_B} + V_A(\vec{r}_A) + V_B(\vec{r}_B) + V_I(\vec{r}_A,\vec{r}_B,\vec{R})]\chi_n(\vec{r}_A,\vec{r}_B,\vec{R})$$

$$= E_n(\vec{R})\chi_n(\vec{r}_A,\vec{r}_B,\vec{R}) \tag{2.3}$$

where $E_n(\vec{R})$ is the energy eigenvalue of Eq. (2.3) and depends parametrically on $\vec{R}$. For each arrangement of the nuclei indexed by $\vec{R}$, there corresponds an electron distribution $|\chi_n(\vec{r}_A,\vec{r}_B,\vec{R})|^2$ with energy $E_n(\vec{R})$. At infinite separation, $E_n(\vec{R})$ corresponds to the sum of the energies of the atomic states.

The eigenfunction, $\chi_n(\vec{r}_A,\vec{r}_B,\vec{R})$, is the molecular wave function of the state n and depends parametrically on $\vec{R}$. Also, the molecular wave functions form a complete orthonormal set for the electronic

variables and can be used as a basis for an expansion of the wave function of the entire system. That is

$$\Psi(\vec{r}_A, \vec{r}_B, \vec{R}) = \sum_n \chi_n(\vec{r}_A, \vec{r}_B, \vec{R}) \, F_n(\vec{R}) \qquad (2.4)$$

Substituting Eq. (2.4) into Eq. (2.1) and multiplying by χ_n^* and integrating over all electronic coordinates gives

$$[- \frac{1}{2M} \nabla_{\vec{R}}^2 + U(\vec{R}) + E_n(\vec{R}) - E] \, F_n(\vec{R})$$

$$= \frac{1}{2M} \sum_{n'} \{2[\overrightarrow{\nabla_{\vec{R}} F_{n'}}(\vec{R})] \cdot \int d\vec{r}_A \, d\vec{r}_B \, \chi_n^* \, \overrightarrow{\nabla_{\vec{R}} \chi_{n'}}$$

$$+ F_{n'}(\vec{R}) \int d\vec{r}_A \, d\vec{r}_B \, \chi_n^* \, \nabla_{\vec{R}}^2 \chi_{n'} \} . \qquad (2.5)$$

The complete quantum treatment would require the solution of Eq. (2.5). Then from the asymptotic form of $F_n(\vec{R})$ the phase shifts can be found and consequently the cross sections for the various processes can be found.

In general, the solution of Eq. (2.5) is very difficult. However, a semi-classical approach, which combines time dependent perturbation theory and a classical trajectory, is used. That is, the electrons may be considered to move in a time dependent potential, the time dependence arising from the motion of the nuclei. The wave equation for the electrons is

$$H_{e\ell} \, \phi(\vec{r}_A, \vec{r}_B, \vec{R}(t)) = i \frac{\partial}{\partial t} \phi(\vec{r}_A, \vec{r}_B, \vec{R}(t)) \qquad (2.6)$$

where $H_{e\ell}$ is given by the left hand side of Eq. (2.3) and the $\frac{\partial}{\partial t}$ is to be performed with $\vec{r}_A$ and $\vec{r}_B$ constant. Since the internuclear distance is a function of time, an approximate solution of Eq. (2.6) is

$$\phi_n = \chi_n(\vec{r}_A,\vec{r}_B,\vec{R}(t))\exp[-i\int^t E_n(\vec{R}(t))dt] \qquad (2.7)$$

where the molecular wave function, χ_n, is assumed to vary slowly with respect to $\vec{R}$. The full wave function can be expanded in terms of the basis functions, Eq. (2.7), to give

$$\phi(\vec{r}_A,\vec{r}_B,\vec{R}(t)) = \sum_n a_n(t)\phi_n(\vec{r}_A,\vec{r}_B,\vec{R}(t)) \qquad (2.8)$$

where a_n is the transition amplitude. Substituting Eq. (2.8) into Eq. (2.6), a set of coupled differential equations for the a's results. A solution of the differential equations can be found by assuming a straight line path and that the velocity is constant. This method is very similar to the multistate impact parameter method which will be discussed later.

Both the quantum and the semi-classical treatment have the same failings. One is that the electronic eigenfunctions do not allow for the rotation of the internuclear line and the other is that the translational motion of the electrons with respect to the center of mass is not accounted for.

Corrections have been made to improve this method. The perturbed rotating atom (PRA) approximation was proposed by Bates[16] to allow for the rotation of the internuclear line during the collision. In

this method the eigenfunctions of the quasimolecule are replaced by
the eigenfunctions of the target perturbed by the projectile. The
axis of quantization is changed from the internuclear line to an axis
parallel to the initial trajectory. An impact parameter formalism
similar to the semi-classical method mentioned before is used.
However, Bates[16] has pointed out that allowing for the rotation of
the internuclear line shows that strong couplings exist between
states whose quantum numbers are identical except for the magnetic
quantum numbers. Also he noted that strong couplings will exist to
states whose potential energy surfaces are close to the states of
interest. An expansion of the wave function must be made over
several states which results in a complicated set of equations that
must be solved.

A traveling molecular wave function was used to correct for the
translational motion of the electron. The basis functions were
changed by the multiplication of the molecular wave function by a
plane wave that represents the translational motion of the electrons.
However, the addition of this factor spoils the effectiveness of the
expansion, Eq. (2.4). The main drawback is that the form used forces
the electron to belong to one center or the other when for slow
collisions the electron belongs to neither center. Also the
integrals in Eq. (2.5) become more difficult to do since some will
contain plane waves.

As long as the collisions are very slow, the difficulties
mentioned are minimal and calculations are possible. However, if
the collisions become too energetic, a correct calculation becomes

unfeasible. The methods mentioned here can not be easily modified to use for collisions in the intermediate energy range.

B. High Energy

For collisions at high energy, the first Born approximation is used exclusively. This approximation assumes that the projectile energy is high enough that the kinetic energy term of the Hamiltonian of Eq. (2.1) is dominant and the interaction potential V can be treated as a perturbation. The zero order equation can be solved in terms of a plane wave multiplied by a product of atomic wave functions. That is

$$[- \frac{1}{2M} \nabla^2_{\vec{R}} - \frac{1}{2} \nabla^2_{\vec{r}_A} - \frac{1}{2} \nabla^2_{\vec{r}_B} + V_A(\vec{r}_A) + V_B(\vec{r}_B)]\phi_n(\vec{r}_A,\vec{r}_B,\vec{R})$$

$$= \epsilon_n \phi_n(\vec{r}_A,\vec{r}_B,\vec{R}) \ . \tag{2.9}$$

The solution of Eq. (2.9) is

$$\phi_n = (2\pi)^{-\frac{3}{2}} e^{i\vec{K}\cdot\vec{R}} \phi_A(\vec{r}_A)\phi_B(\vec{r}_B) \tag{2.10}$$

and

$$\epsilon_n = \frac{k^2}{2M} + \epsilon_A + \epsilon_B \tag{2.11}$$

where $\phi_A(\vec{r}_A)$ and $\phi_B(\vec{r}_B)$ are the atomic wave functions and ϵ_A and ϵ_B are the internal energies of the atoms. The perturbation V is taken to be the interaction between atoms A and B. That is

$$V(\vec{r}_A, \vec{r}_B, \vec{R}) = V_I(\vec{r}_A, \vec{r}_B, \vec{R}) + U(\vec{R}) . \qquad (2.12)$$

The Born approximation is so commonly used and can be found in almost any quantum mechanics book that a long discussion is unnecessary.[20] Eqs. (2.9)-(2.12) show how the Hamiltonian is arranged for the particular case of atom-atom collisions.

The simplicity of this method makes it very inviting for modification for the intermediate energy range. The eikonal DWBA is a modification of the Born approximation and will be discussed later.

C. Intermediate Energy

1. The Multistate Impact Parameter Method

The multistate impact parameter method assumes that the collision is at a high enough energy that the change in kinetic energy due to inelastic scattering is so small that the change can be neglected and the kinetic energy is assumed to be constant. Also small angle scattering is assumed, so the change in momentum can be neglected and the trajectory is taken as a straight line. A brief discussion of the method will be given. A more complete description is given elsewhere.[21]

The projectile, atom A, travels along a straight line with a constant velocity v. The trajectory is parallel to the Z axis, the axis of quantization for both atoms, and remains a distance b, the impact parameter, from the Z axis. The origin of this cylindrical coordinate system is placed at the target atom B. The internuclear

separation is $\vec{R}$ and the electron positions with respect to the atoms A and B are labeled $\vec{r}_A$ and $\vec{r}_B$. In this approximation the electronic wave function for the system is given by

$$\Psi(\vec{r}_A,\vec{r}_B,t) = \sum_m a_m(t) \; \psi_m(\vec{r}_A,\vec{r}_B) e^{-iE_m t} \qquad (2.13)$$

where ψ_m is the product of the projectile wave function $\phi_A(\vec{r}_A)$ and the target wave function $\phi_B(\vec{r}_B)$; E_m is the sum of the electronic energies ε_A and ε_B; and the transition amplitude is a_m.

Using the wave function of Eq. (2.13) and the interaction potential of Eq. (2.12) as a time dependent perturbation, an infinite set of first order coupled differential equations is obtained for the transition amplitudes. The result is

$$i \; \frac{\partial a_n(t)}{\partial t} = \sum_m a_m(t) \; V_{nm}(\vec{R}(t)) e^{iE_{nm} t} \qquad (2.14)$$

where

$$E_{nm} = E_n - E_m \qquad (2.15)$$

and

$$R = (b^2 + v^2 t^2)^{\frac{1}{2}} \; . \qquad (2.16)$$

The matrix element is given by

$$V_{nm} = \langle \psi_n(\vec{r}_A,\vec{r}_B) | V(\vec{R}(t),\vec{r}_A,\vec{r}_B) | \psi_m(\vec{r}_A,\vec{r}_B) \rangle \; . \qquad (2.17)$$

In practice, the series is truncated and a finite set of N coupled differential equations is solved. The probability of the transition from the initial state 1 to the final state n is given by

$$P_{1n}^{N}(b) = |a_n(+\infty)|^2 .$$ (2.18)

The total excitation cross section for a particular velocity v is given by

$$\sigma_{1n} = 2\pi \int_0^\infty P_{1n}^{N}(b) \, b \, db .$$ (2.19)

The solution of the N coupled differential equations and the evaluation of the cross sections are carried out numerically.

This method allows for the distortion of the plane wave and also for the couplings between states. The assumption that the projectile travels in a straight line throughout the collision eliminates the possibility of calculating a differential cross section. Both the total and differential cross sections can be calculated in the eikonal DWBA.

2. The Eikonal Approximation

The eikonal approximation is a common approximation used in physics. In nuclear physics, the Glauber approximation[22] is the eikonal method applied to nuclear scattering. In 1968, Franco[23], using the formalism of the Glauber approximation, was the first to apply this method to electron-atom scattering. The basic idea of the

approximation is that the wave function, Eq. (2.10), is modified by a factor $\exp[S(\vec{R})]$ where $S(\vec{R})$ is a slowly varying function of $\vec{R}$. That is, for atom-atom collisions the wave function is

$$\phi_n(\vec{r}_A,\vec{r}_B,\vec{R}) = (2\pi)^{-\frac{3}{2}} e^{i\vec{k}_i\cdot\vec{R}} \phi_A(\vec{r}_A)\phi_B(\vec{r}_B)e^{S(\vec{R})} \quad . \tag{2.20}$$

Substitution of the modified wave function, Eq. (2.20), back into the wave equation, Eq. (2.1), will give the following equation for $S(\vec{R})$.

$$[2i\vec{k}_i\cdot\overrightarrow{\nabla_{\vec{R}}S}(\vec{R}) + \nabla^2_{\vec{R}}S(\vec{R}) + (\nabla_{\vec{R}}S(\vec{R}))^2 - 2MV(\vec{R},\vec{r}_A,\vec{r}_B)] = 0 \tag{2.21}$$

Since $S(\vec{R})$ is a slowly varying function of $\vec{R}$, the first term of Eq. (2.21) dominates and the other terms are neglected. The initial momentum $\vec{k}_i$ is assumed to be along the Z axis. The solution for $S(\vec{R})$ in the Glauber approximation is

$$S(\vec{R}) = -\frac{i}{v} \int_{-\infty}^{Z} V(\vec{R}',\vec{r}_A,\vec{r}_B)dZ' \tag{2.22}$$

The cross section can be found by using the modified wave function, Eq. (2.20), in the scattering amplitude.

$$f_{fi}(\vec{q}) = \frac{-M}{(2\pi)} \iiint e^{i\vec{q}\cdot(\vec{b}+\hat{Z}Z)} \phi^*_{A_f}(\vec{r}_A)\phi^*_{B_f}(\vec{r}_B)\exp[-\frac{i}{v}\int_{-\infty}^{Z} V(\vec{R}',\vec{r}_A,\vec{r}_B)dZ']$$

$$V(\vec{R},\vec{r}_A,\vec{r}_B) \phi_{A_i}(\vec{r}_A) \phi_{B_i}(\vec{r}_B) d\vec{R} d\vec{r}_A d\vec{r}_B \tag{2.23}$$

where i and f label the initial and final states and the momentum transfer is

$$\vec{q} = \vec{k}_i - \vec{k}_f \tag{2.24}$$

and

$$\vec{R} = \vec{b} + Z\hat{Z} \ . \tag{2.25}$$

In the limit of high energies and small angle scattering, the momentum transfer is assumed to be perpendicular to the initial momentum. This allows the Z integrand to be written as a total derivative and therefore the Z integration can be easily done.

This approximation has been applied to e-H scattering by Franco[23]; and Bhadra and Ghosh[24]; and Tai, Bassel, Gerjuoy, and Franco[25]. Also e-He calculations by Franco[26] and by Yates and Tenney[27] demonstrated that this is a promising method.

However, there does exist some valid criticism of the Glauber approximation. The scattering amplitude is a multidimensional integral over electron coordinates and the internuclear coordinates. The assumption that the momentum transfer was perpendicular to the initial momentum causes an unphysical selection rule. Thus, the $1s \rightarrow 2p_0$ excitation cross section of H in the e-H collision is identically zero.

Byron[28] has done a modified Glauber calculation for e-H and e-He scattering in which no restrictions were placed on the momentum transfer. The 6-dimensional integral for e-H scattering and the 9-dimensional integral for e-He scattering were performed

numerically using the Monte Carlo method. For e-H scattering, the
1s→2s excitation cross sections of Byron agree virtually exactly
with the calculation of Tai, et al.[25] Byron's[28] value for the
1s→2p$_0$ excitation was, of course, non-zero. The relative population
of the magnetic substates of the 2p level of hydrogen gives rise
to the polarization of the emitted radiation after the collision.
The calculation of Tai, et al.[25] yields a constant negative polari-
zation. Byron's[28] calculation gives a positive polarization that
agrees fairly well with the experimental results.

The number of integrals that can be done analytically depends
upon the form of the interaction potential as well as the form of
the atomic wave function. Franco[29] has shown that for electron
scattering off an atom with Z electrons the (3Z+2) dimensional
integrals for the scattering amplitude can be reduced to a one
dimensional integral to be performed numerically. However, his
derivation is limited by the assumptions that the atomic wave function
could be represented as a product of particular functions of one
electron coordinate and that the interaction potential is a sum of
coulomb terms that contain only one electron coordinate. This
permits the integrals over the electronic coordinates to be factored
out and done separately. However, for atom-atom collisions the inter-
action potentials contain terms that mix the electronic coordinates,
so that the procedure used for electron-atom collisions is not
applicable to atom-atom collisions. The large number of integrals
to be done numerically makes this method unfeasible for atom-atom
collisions.

The eikonal distorted wave Born approximation is very similar to the Glauber approximation, but manages to avoid the same criticism. The eikonal DWBA results in a three dimensional integral to be done no matter how many electrons are involved. Also no selection rule occurs for the $1s \rightarrow 2p_O$ excitation. The derivation of the eikonal DWBA will be given in the next section.

III. THE EIKONAL DISTORTED WAVE BORN APPROXIMATION

Consider the nonrelativistic rearrangement collision

$$A + B \rightarrow C + D \qquad (3.1)$$

where A, B, C, and D can be elementary or composite particles with masses M_A, M_B, M_C, and M_D. The center of mass coordinate system is used where $\vec{R}_i$ and $\vec{k}_i$ are the relative coordinate and relative momentum, respectively, for particles A and B in the initial channel i. The reduced mass M_i in the initial channel is given by

$$M_i^{-1} = M_A^{-1} + M_B^{-1} \qquad (3.2)$$

The initial channel Hamiltonian H_i is

$$H_i = K_i + h_i \qquad (3.3)$$

where K_i is the relative kinetic energy operator given by

$$K_i = -(2M_i)^{-1} \nabla_{\vec{R}_i}^2 \qquad (3.4)$$

The internal Hamiltonian of the initial channel satisfies

$$h_i \phi_\alpha(\xi_i) = \varepsilon_\alpha \phi_\alpha(\xi_i) \qquad (3.5)$$

The subscript α refers to a collection of quantum numbers and ξ_i denotes a set of generalized coordinates describing the internal structure of the systems A and B. If h_A and h_B are the internal Hamiltonians of A and B with

$$h_A \phi_A(\vec{r}_A) = \varepsilon_A \phi_A(\vec{r}_A) \tag{3.6}$$

and

$$h_B \phi_B(\vec{r}_B) = \varepsilon_B \phi_B(\vec{r}_B) \quad , \tag{3.7}$$

then

$$h_i = h_A + h_B \tag{3.8}$$

and

$$\varepsilon_\alpha = \varepsilon_A + \varepsilon_B \tag{3.9}$$

and

$$\phi_\alpha(\xi_i) = \phi_A(\vec{r}_A)\phi_B(\vec{r}_B) \tag{3.10}$$

The total energy in the center of mass in channel i is

$$E_a \equiv E_{i,\alpha} = \frac{k_i^2}{2M_i} + \varepsilon_A + \varepsilon_B = \frac{k_i^2}{2M_i} + \varepsilon_\alpha \tag{3.11}$$

where the notation $a \equiv (i,\alpha)$. The channel eigenfunction or asymptotic states $\chi_a = \chi_{i,\alpha}$ are solutions to

$$H_i \chi_a = E_a \chi_a \tag{3.12}$$

where χ_a is

$$\chi_a(\vec{R}_i,\xi_i) = (2\pi)^{-\frac{3}{2}} e^{i\vec{k}_i \cdot \vec{R}_i} \phi_\alpha(\xi_i) \tag{3.13}$$

If the interaction between systems A and B is denoted by V_i the total Hamiltonian is

$$H = H_i + V_i \qquad (3.14)$$

A similar set of equations hold in the final channel with the substitutions i→f, α→β, A→C, and B→D.

Let us suppose that the scattering proceeds from an initial state χ_a to a final state χ_b. The differential cross section for this process is given by

$$\frac{d\sigma}{d\Omega} = (2\pi)^4 (k_f/k_i) M_i M_f |T_{ba}|^2 \qquad (3.15)$$

where T_{ba} is the T matrix on the energy-momentum shell. The T matrix can be written as

$$T_{ba} = \langle \chi_b | V_f | \psi_a^+ \rangle = \langle \psi_b^- | V_i | \chi_a \rangle . \qquad (3.16)$$

The ψ_a^+ and ψ_b^- are state vectors given by

$$\psi_a^+ = \chi_a + (E-H+i\eta)^{-1} V_i \chi_a \qquad (3.17)$$

and

$$\psi_b^- = \chi_b + (E-H-i\eta)^{-1} V_f \chi_b \qquad (3.18)$$

with $\eta \to 0^+$.

The equations given above are common to the theory of rearrangement collisions. For example, see Geltman[30] for a general treatment of rearrangement collisions.

Let us suppose that the interaction potentials are decomposed in the initial and final channels as

$$V_i = U_i + W_i \tag{3.19}$$

and

$$V_f = U_f + W_f \tag{3.20}$$

where U_i and U_f are potentials that we wish to take into account directly in the channel eigenfunction. New Hamiltonians can be defined as

$$\tilde{H}_i = H_i + U_i \tag{3.21}$$

and

$$\tilde{H}_f = H_f + U_f \tag{3.22}$$

The corresponding state vectors are

$$\phi_a^+ = \chi_a + (E - \tilde{H}_i + i\eta)^{-1} U_i \chi_a \tag{3.23}$$

and

$$\phi_b^- = \chi_b + (E - \tilde{H}_f - i\eta)^{-1} U_f \chi_b \tag{3.24}$$

with $\eta \rightarrow 0^+$.

The state vectors, ϕ_a^+ and ϕ_b^-, can be incorporated into the theory by means of the T matrix. A simple calculation yields the T matrix for scattering from two potentials.[31] That is

$$T_{ba} = \langle \chi_b | V_f - W_i | \phi_a^+ \rangle + \langle \psi_b^- | W_i | \phi_a^+ \rangle . \tag{3.25}$$

Also

$$T_{ba} = \langle \phi_b^- | V_i - W_f | \chi_a \rangle + \langle \phi_b^- | W_f | \psi_a^+ \rangle . \tag{3.26}$$

A physically meaningful separation of V_i and V_f is to choose U_i and U_f so that they induce elastic scattering. That may be accomplished if the choice is

$$U_i = U_i(\vec{R}_i) \tag{3.27}$$

$$U_f = U_f(\vec{R}_f) \tag{3.28}$$

The state vectors are just the distorted waves. The T matrices of Eqs. (3.25) and (3.26) reduce to

$$T_{ba} = \langle \psi_b^- | W_i | \phi_a^+ \rangle \tag{3.29}$$

$$T_{ba} = \langle \phi_b^- | W_f | \psi_a^+ \rangle \tag{3.30}$$

The above equations are still rigorous. However an approximation is needed to obtain results. Let

$$\psi_a^+ \simeq \phi_a^+ \tag{3.31}$$

and

$$\psi_b^- \simeq \phi_b^- . \tag{3.32}$$

The total wave function is being approximated by the distorted wave. The T matrix becomes, in the distorted wave Born approximation (DWBA),

$$T_{ba}^{DWBA} = \langle \phi_b^- | W_f | \phi_a^+ \rangle = \langle \phi_b^- | W_i | \phi_a^+ \rangle \tag{3.33}$$

The choices of the potentials U_i and U_f have only been restricted to be a function of the internuclear coordinates and not of the electronic coordinates. However, the best choice for U_i and U_f are the optical potentials[32] describing the elastic scattering in the initial and final channels. The scattering reaction consists of an incoming wave whose phase has been distorted by the elastic potential U_i; a single interaction is induced by W_i or W_f; and the outgoing plane wave is distorted by the elastic potential U_f.

A straight line eikonal approximation can be used to approximate ϕ_a^+ and ϕ_b^-. This approximation assumes a solution for the initial channel as

$$\phi_a^+ = (2\pi)^{-\frac{3}{2}} \exp[i\vec{k}_i \cdot \vec{R}_i + S(\vec{R}_i)] \; \phi_\alpha(\xi_i) \qquad (3.34)$$

and that $S(\vec{R}_i)$ is a slowly varying function. Substitution of Eq. (3.34) into the wave equation with the Hamiltonian $\tilde{H}_i$, Eq. (3.21), will give an equation for $S(\vec{R}_i)$ similar to Eq. (2.21) except $V(\vec{R},\vec{r}_A,\vec{r}_B)$ will be changed to $U_i(\vec{R}_i)$. Since $S(\vec{R}_i)$ is slowly varying, only the term with the single derivative will be kept. The direction for $\vec{k}_i$ can be taken along the Z axis. This allows $S(\vec{R}_i)$ to be easily solved for and be written as

$$S(\vec{R}_i) = -\frac{i}{v_i} \int_{-\infty}^{Z_i} U_i(\vec{b}_i,Z_i')dZ_i' \quad . \qquad (3.35)$$

where

$$\vec{R}_i = \vec{b}_i + \hat{Z}Z_i \quad \text{and} \quad v_i = k_i/M_i \quad . \qquad (3.36)$$

A similar procedure can be followed in the final channel. The distorted waves in the eikonal approximation are

$$\phi_a^{+(eik)} = (2\pi)^{-\frac{3}{2}} \exp[i\vec{k}_i \cdot \vec{R}_i - \frac{i}{v_i} \int_{-\infty}^{Z_i} U_i(\vec{b}_i, Z_i')dZ_i']\phi_\alpha(\xi_i) \qquad (3.37)$$

and

$$\phi_b^{-(eik)} = (2\pi)^{-\frac{3}{2}} \exp[i\vec{k}_f \cdot \vec{R}_f - \frac{i}{v_f} \int_{\infty}^{Z_f} U_f(\vec{b}_f, Z_f')dZ_f']\phi_\beta(\xi_f) \qquad (3.38)$$

For direct collisions where rearrangement does not occur, the subscript of i or f on the electronic and internuclear coordinates can be dropped. Substituting the distorted waves, Eqs. (3.37) and (3.38), into $T_{ba}^{(DWBA)}$, Eq. (3.33), the T matrix in the eikonal DWBA[14] becomes

$$T_{ba}^{(eik)} = (2\pi)^{-3} \int_0^\infty db\ b \int_{-\infty}^\infty dZ \int_0^{2\pi} d\phi\ \exp[i(k_i - k_f\cos\theta)Z$$

$$+ i\delta\phi(\vec{b},Z) - ik_f b\ \sin\theta\ \cos\phi]A(\vec{b},Z) \qquad (3.39)$$

where

$$\delta\phi(\vec{b},Z) = -\frac{1}{v_i} \int_{-\infty}^Z U_i(\vec{b},Z')dZ' - \frac{1}{v_f} \int_Z^\infty U_f(\vec{b},Z')dZ' \qquad (3.40)$$

and

$$A(\vec{b},Z) = <\phi_\beta(\xi)|W(\vec{R},\xi)|\phi_\alpha(\xi)> \qquad (3.41)$$

IV. EXCITATION TO THE 2s AND 2p STATES OF HYDROGEN BY HYDROGEN IMPACT

A. Basic Equations

The eikonal distorted wave Born approximation has been applied to the process given by Eq. (1.2) in the energy range of 2.25 keV (v = .3 a.u.) to 100 keV (v = 2.0 a.u.).

The interaction potential was taken as

$$V(\vec{R},\vec{r}_{1A},\vec{r}_{2B}) = \frac{1}{R} + \frac{1}{|\vec{R}+\vec{r}_{1A}-\vec{r}_{2B}|} - \frac{1}{|\vec{R}+\vec{r}_{1A}|} - \frac{1}{|\vec{R}-\vec{r}_{2B}|} \tag{4.1}$$

where $\vec{r}_{1A}$ and $\vec{r}_{2B}$ are the distances to the electrons from their respective nuclei.

The optical potentials are approximated by the corresponding static potentials and the elastic matrix elements are

$$U_i = \langle\phi_{1s}(\vec{r}_{1A})\phi_{1s}(\vec{r}_{2B})|V(\vec{R},\vec{r}_{1A},\vec{r}_{2B})|\phi_{1s}(\vec{r}_{1A})\phi_{1s}(\vec{r}_{2B})\rangle$$

$$= \frac{e^{-2R}}{24} \left(\frac{24}{R} + 15 - 18R - 4R^2\right) \; , \tag{4.2}$$

$$U_f^{2s} = \langle\phi_{1s}(\vec{r}_{1A})\phi_{2s}(\vec{r}_{2B})|V(\vec{R},\vec{r}_{1A},\vec{r}_{2B})|\phi_{1s}(\vec{r}_{1A})\phi_{2s}(\vec{r}_{2B})\rangle$$

$$= \frac{1}{81} \left[e^{-R}\left(\frac{209}{R} - \frac{669}{4} + \frac{225R}{4} - \frac{63R^2}{8}\right) + e^{-2R}\left(-\frac{128}{R} + 36\right)\right] \; , \tag{4.3}$$

$$U_f^{2p_0} = <\phi_{1s}(\vec{r}_{1A})\phi_{2p_0}(\vec{r}_{2B})|V(\vec{R},\vec{r}_{1A},\vec{r}_{2B})|\phi_{1s}(\vec{r}_{1A})\phi_{2p_0}(\vec{r}_{2B})>$$

$$= U_0(R) + (3\frac{Z^2}{R^2} - 1)U_2(R) \quad , \tag{4.4}$$

and

$$U_f^{2p_+} = <\phi_{1s}(\vec{r}_{1A})\phi_{2p_+}(\vec{r}_{2B})|V(\vec{R},\vec{r}_{1A},\vec{r}_{2B})|\phi_{1s}(\vec{r}_{1A})\phi_{2p_+}(\vec{r}_{2B})>$$

$$= U_0(R) - \frac{1}{2}(3\frac{Z^2}{R^2} - 1)U_2(R) \quad , \tag{4.5}$$

where

$$U_0 = \frac{1}{1944}[e^{-R}(\frac{664}{R} - 558 + 198R - 63R^2) + e^{-2R}(\frac{1280}{R} + 1824)] \tag{4.6}$$

and

$$U_2 = \frac{1}{1944}[e^{-R}(\frac{912}{R^3} + \frac{912}{R^2} - \frac{56}{R} - 360 + 198R - 63R^2)$$

$$- 16e^{-2R}(\frac{57}{R^3} + \frac{114}{R^2} + \frac{82}{R} + 12)] \quad . \tag{4.7}$$

The off diagonal matrix elements are given by

$$A_{2s}(\vec{R}) = <\phi_{1s}(\vec{r}_{1A})\phi_{2s}(\vec{r}_{2B})|V(\vec{R},\vec{r}_{1A},\vec{r}_{2B})|\phi_{1s}(\vec{r}_{1A})\phi_{1s}(\vec{r}_{2B})>$$

$$= \frac{4\sqrt{2}}{2401}[e^{-\frac{3R}{2}}(\frac{12288}{R} - 4403 + \frac{1127R}{2}$$

$$- e^{-2R}(\frac{12288}{R} + 1792)] \quad , \tag{4.8}$$

$$A_{2p_0}(\vec{R}) = <\phi_{1s}(\vec{r}_{1A})\phi_{2p_0}(\vec{r}_{2B})|V(\vec{R},\vec{r}_{1A},\vec{r}_{2B})|\phi_{1s}(\vec{r}_{1A})\phi_{1s}(\vec{r}_{2B})>$$

$$= (Z/R)A_0(R) \quad , \tag{4.9}$$

and

$$A_{2p_+}(\vec{R}) = <\phi_{1s}(\vec{r}_{1A})\phi_{2p_+}(\vec{r}_{2B})|V(\vec{R},\vec{r}_{1A},\vec{r}_{2B})|\phi_{1s}(\vec{r}_{1A})\phi_{1s}(\vec{r}_{2B})>$$

$$= \frac{-b}{\sqrt{2}\ R}\ e^{i\phi}\ A_0(R) \tag{4.10}$$

where

$$A_0 = \frac{48\sqrt{2}}{2401}\ [e^{-\frac{3R}{2}}(\frac{440}{R^2} + \frac{660}{R} - 273 + \frac{1127R}{24})$$

$$- 8e^{-2R}(\frac{55}{R^2} + \frac{110}{R} + 14)] \quad . \tag{4.11}$$

The ϕ integration in the T matrix, Eq. (3.39) can be performed and the J_0 or J_1 Bessel function will result. The T matrix elements can be written as

$$T_{2s,1s}^{(eik)} = (2\pi^2)^{-1} \int_0^\infty db\ b\ J_0(b\ k_f\ \sin\theta)\ \exp[i\phi^{2s}(b)]$$

$$\int_0^\infty A_{2s}(b,Z)\ \cos[(k_i-k_f\ \cos\theta)Z + \gamma^{2s}(b,Z)]dZ \tag{4.12}$$

where

$$\phi^{2s}(b) = \int_0^\infty (-U_i(b,Z)/v_i - U_f^{2s}(b,Z)/v_f)\ dZ \tag{4.13}$$

and

$$\gamma^{2s}(b,Z) = \int_0^Z (-U_i(b,Z')v_i + U_f^{2s}(b,Z')/v_f) \, dZ' \quad . \qquad (4.14)$$

Also,

$$T_{2p_o,1s}^{(eik)} = \frac{i}{(2\pi^2)} \int_0^\infty db \, b \, J_0(b \, k_f \, \sin\theta) \, \exp[i \, \phi^{2p_o}(b)]$$

$$\int_0^\infty A_{2p_o}(b,Z) \, \sin[(k_i-k_f \cos\theta)Z + \gamma^{2p_o}(b,Z)]dZ \qquad (4.15)$$

where

$$\phi^{2p_o}(b) = \int_0^\infty [-U_i(b,Z)/v_i - U_f^{2p_o}(b,Z)/v_f]dZ \qquad (4.16)$$

and

$$\gamma^{2p_o}(b,Z) = \int_0^Z [-U_i(b,Z')/v_i + U_f^{2p_o}(b,Z')/v_f]dZ' \quad , \qquad (4.17)$$

and finally

$$T_{2p_+,1s}^{(eik)} = \frac{-i}{(2\pi^2)} \int_0^\infty db \, b^2 \, J_1(b \, k_f \, \sin\theta) \, \exp[i \, \phi^{2p_+}(b)]$$

$$\int_0^\infty \frac{A_0(b,Z)}{(\sqrt{2}(b^2+Z^2)^{1/2})} \, \cos[(k_i-k_f \cos\theta)Z + \gamma^{2p_+}(b,Z)] \, dZ \qquad (4.18)$$

where

$$\phi^{2p_+}(b) = \int_0^\infty (-U_i(b,Z)/v_i - U_f^{2p_+}(b,Z)/v_f) \, dZ \tag{4.19}$$

and

$$\gamma^{2p_+}(b,Z) = \int_0^Z (-U_i(b,Z')/v_i + U_f^{2p_+}(b,Z')/v_f) \, dZ' \quad . \tag{4.20}$$

The numerical solutions of the above equations will be discussed in the appendix.

B. Results and Discussion

1. Differential Cross Sections

In Figs. 1-5 the differential cross sections for the 1s→2s excitation are plotted versus the scattering angle θ for the incident velocities v = .3, .4, .5, 1.0, and 2.0 a.u. for both the eikonal DWBA and the first Born approximation. Some general characteristics of the eikonal DWBA can be seen. One consistent observation is that the eikonal DWBA curve lies below the first Born approximation curve for small angles and then crosses the Born curve and remains above it for the larger angles. The eikonal DWBA differential cross sections die off very slowly for large angles. This region of large angle scattering becomes very important when the total cross section is calculated. For example in Fig. 4 for v = 1.0 a.u., the eikonal DWBA curve falls below the Born curve for small angles and then crosses above the Born curve at a scattering angle of $\theta = 2.4 \times 10^{-3}$ rad.

FIG. 1. Differential cross sections for the excitation of

hydrogen to the 2s state by hydrogen impact for an incident velocity

of 0.3 a.u. or for an incident energy of 2.25 keV. The solid line

is the eikonal DWBA and the dashed line is the first Born approxi-

mation. Both the differential cross section and the scattering angle

are given in the center of mass coordinate system.
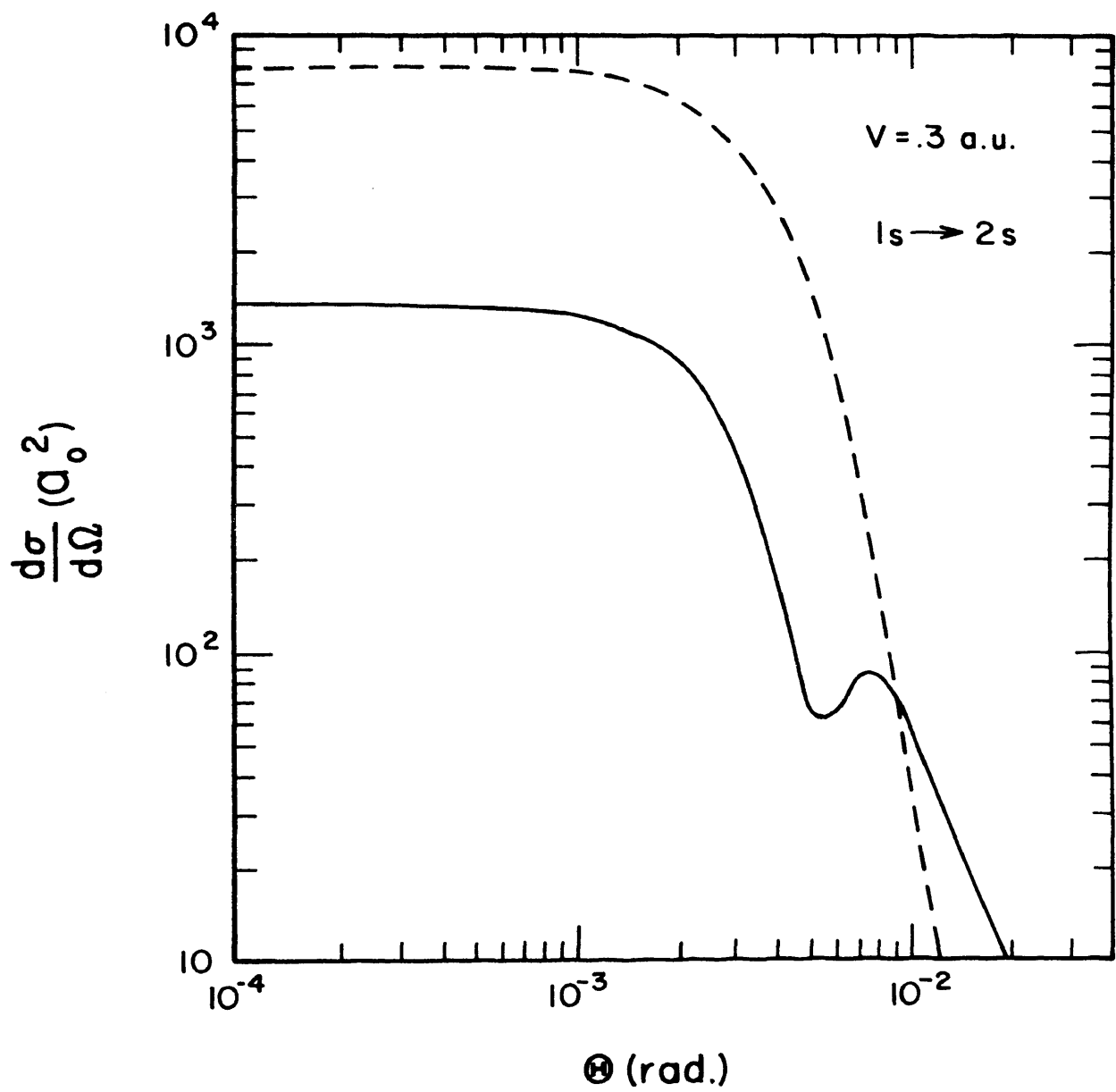
Figure 1

FIG. 2. Differential cross sections for the excitation of hydrogen to the 2s state by hydrogen impact for an incident velocity of 0.4 a.u. or for an incident energy of 4.0 keV. The solid line is the eikonal DWBA and the dashed line is the first Born approximation. Both the differential cross section and the scattering angle are given in the center of mass coordinate system.

Figure 2

34
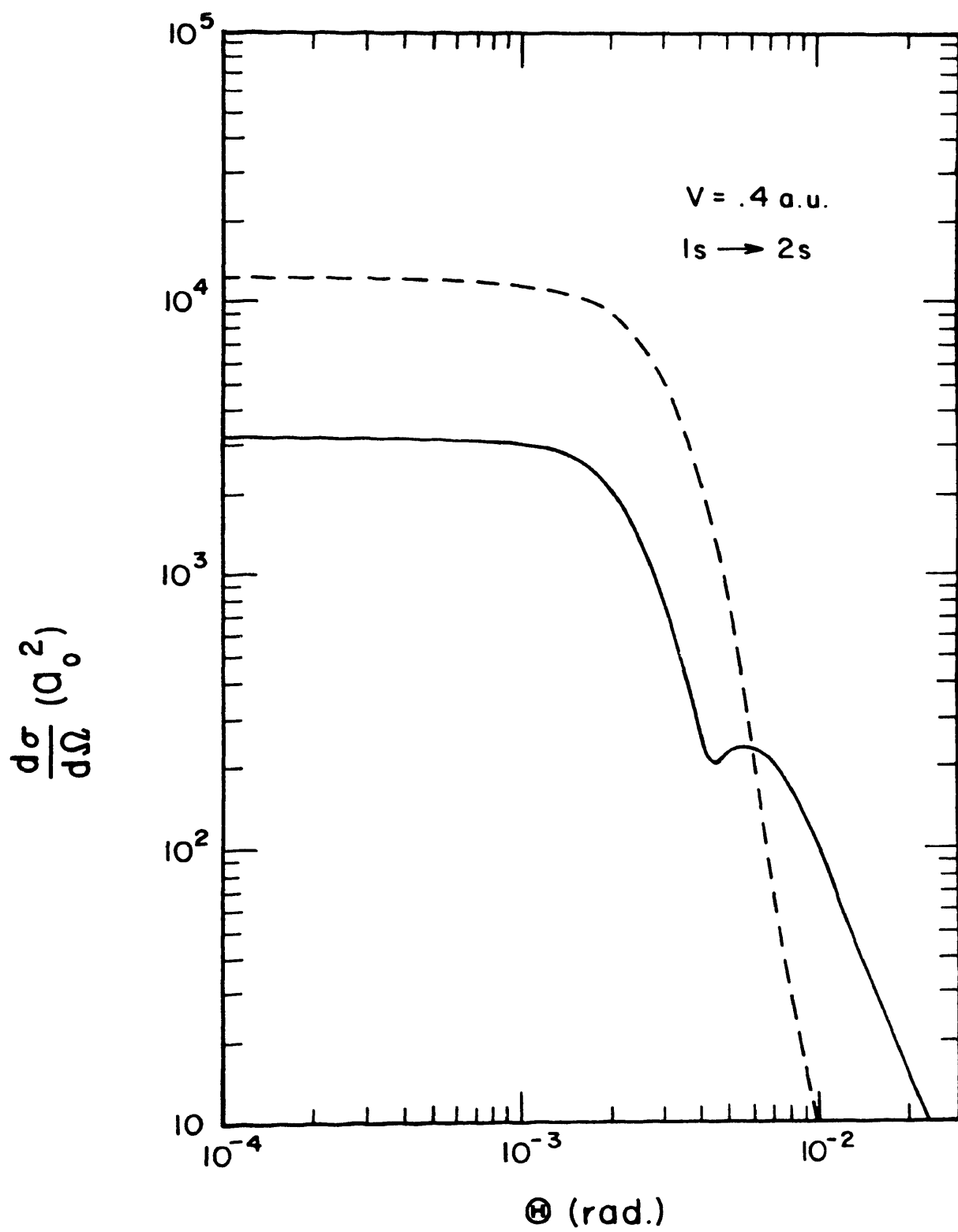
FIG. 3. Differential cross sections for the excitation of hydrogen to the 2s state by hydrogen impact for an incident velocity of 0.5 a.u. or for an incident energy of 6.25 keV. The solid line is the eikonal DWBA and the dashed line is the first Born approximation. Both the differential cross section and the scattering angle are given in the center of mass coordinate system.

Figure 3

FIG. 4. Differential cross sections for the excitation of
hydrogen to the 2s state by hydrogen impact for an incident velocity
of 1.0 a.u. or for an incident energy of 25 keV. The solid line is
the eikonal DWBA and the dashed line is the first Born approximation.
Both the differential cross section and the scattering angle are
given in the center of mass coordinate system.

$$V = 1.0 \text{ a. u.}$$
$$1s \longrightarrow 2s$$

Figure 4

FIG. 5. Differential cross sections for the excitation of
hydrogen to the 2s state by hydrogen impact for an incident velocity
of 2.0 a.u. or for an incident energy of 100 keV. The solid line is
the eikonal DWBA and the dashed line is the first Born approximation.
Both the differential cross section and the scattering angle are
given in the center of mass coordinate system.
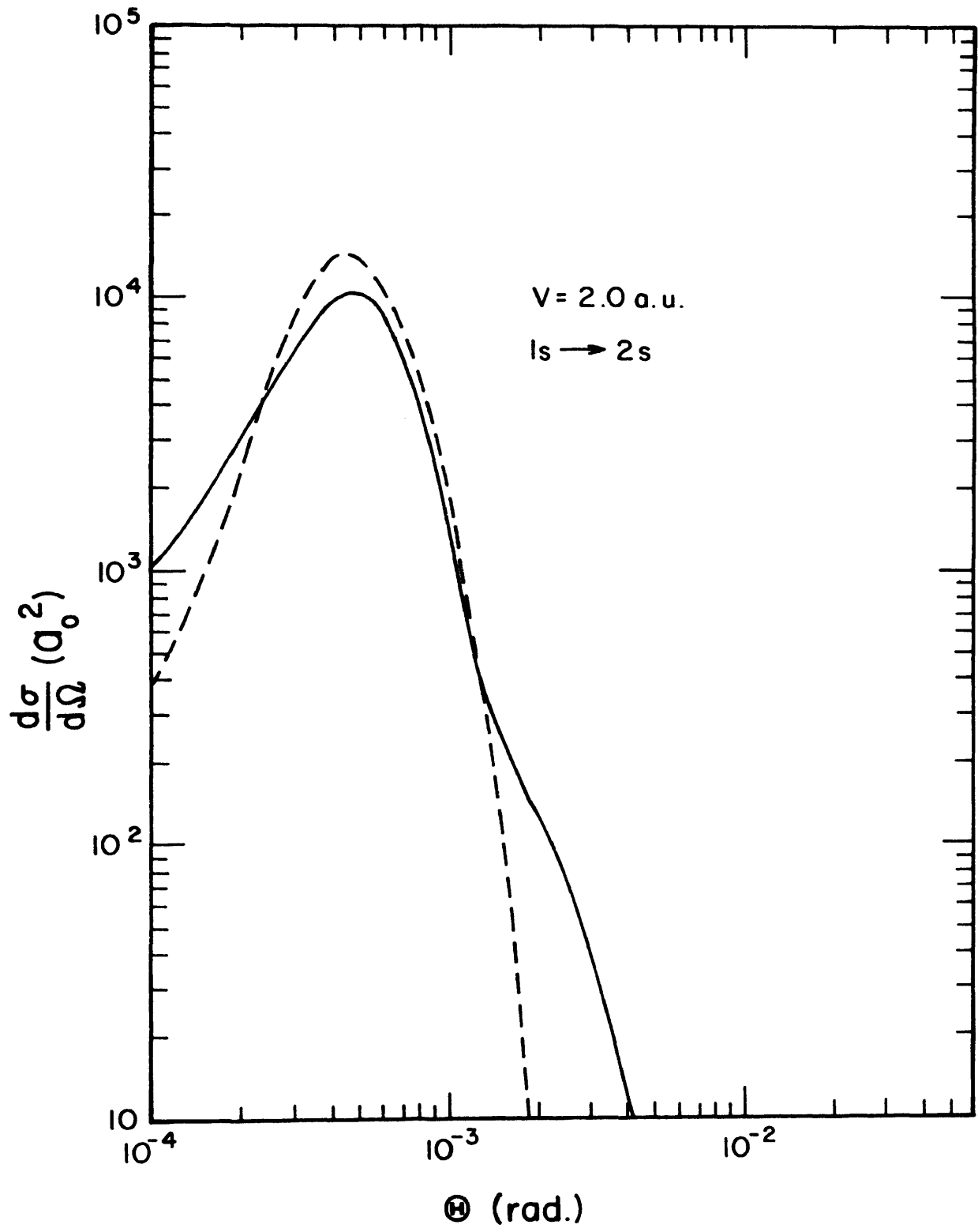
Figure 5

where the differential cross section is a factor of ten below the peak

value. The differential cross section lying outside the crossing

point constitutes 38% of the total cross section for the eikonal DWBA

for this case (v = 1.0 a.u.).

Another characteristic of the eikonal DWBA differential cross

sections is the second peak. The peak is quite sharp in Fig. 1 for

v = .3 a.u. and flattens out for the higher velocities as shown in

Figs. 2-5. For v = 2.0 a.u., Fig. 5, the peak has disappeared and

the difference between the Born and the eikonal DWBA is small.

The physical significance of the second peak is hard to determine.

However, it is due to the interference between the distortion factor

$\exp[i\ \phi(b)]$ and the Bessel function $J_m(b\ k_f\ \sin\theta)$. The result of

the Z integration varies quite slowly with angle and therefore does

not contribute to the second peak. The function $\phi(b)$ behaves as

ln b for small b and as $\exp(-\lambda b)/\sqrt{b}$ for large b. Thus, the factor

$\exp[i\ \phi(b)]$, which is not a function of the scattering angle,

oscillates rapidly for small b and slowly for large b until asymp-

totically the factor equals one. The factor $J_m(b\ k_f\ \sin\theta)$ is also

an oscillating function. The product of these two factors causes the

b integration to be the sum of positive and negative areas. The

areas vary with angle and at a certain angle the sum of the areas

creates a relative minimum in the differential cross sections and at

another angle a relative maximum.

In Figs. 6-10, the differential cross sections for the

$1s \rightarrow 2p_0, 2p_+$ excitations are plotted versus the scattering angle for

v = .3, .4, .5, 1.0, and 2.0 a.u. for both the eikonal DWBA and the

FIG. 6. Differential cross section for the excitation of
hydrogen to the $2p_0$ and $2p_+$ states by hydrogen impact for an incident
velocity of 0.3 a.u. or for an incident energy of 2.25 keV. The
solid line is the eikonal DWBA and the dashed line is the first Born
approximation. Both the differential cross section and the scattering
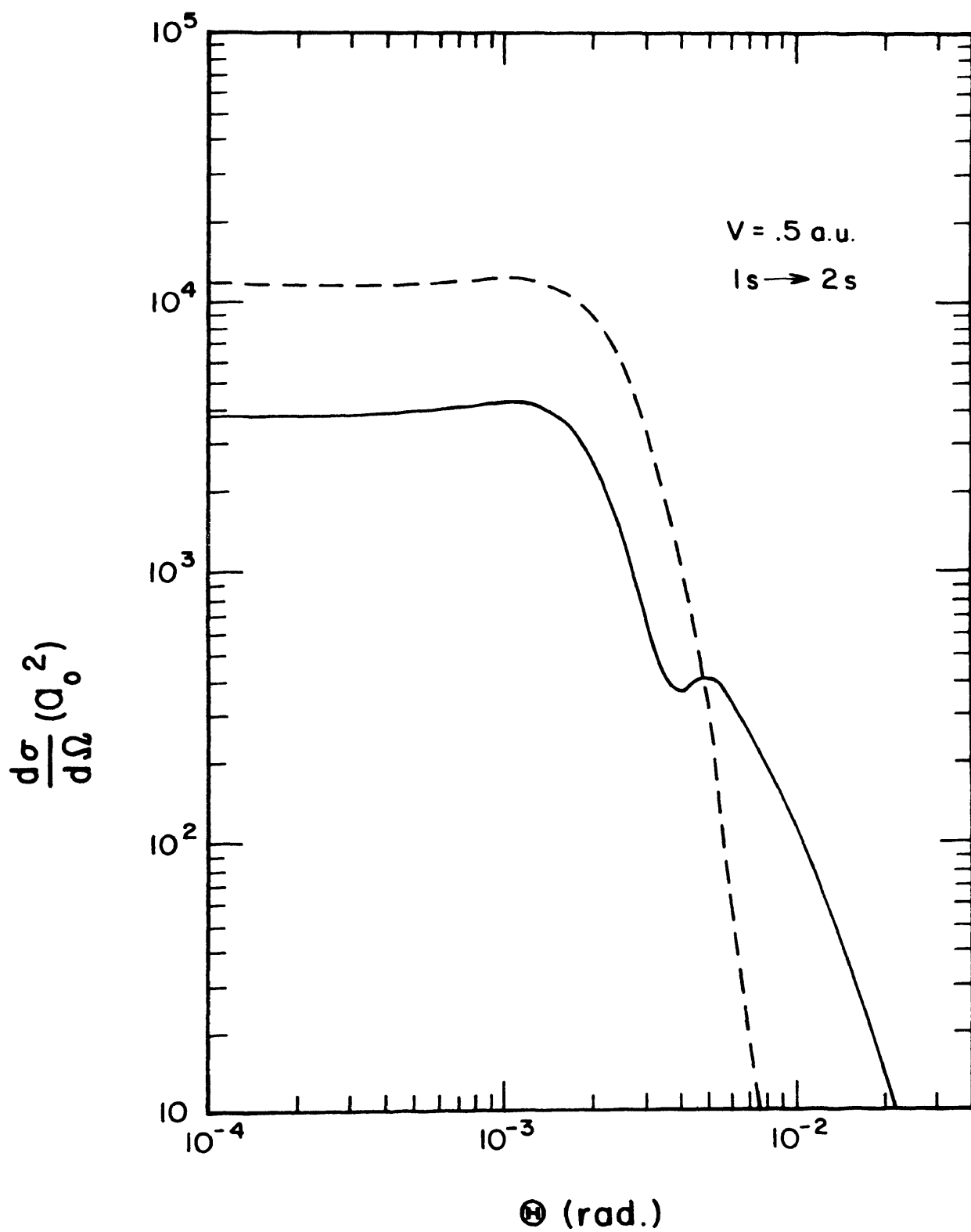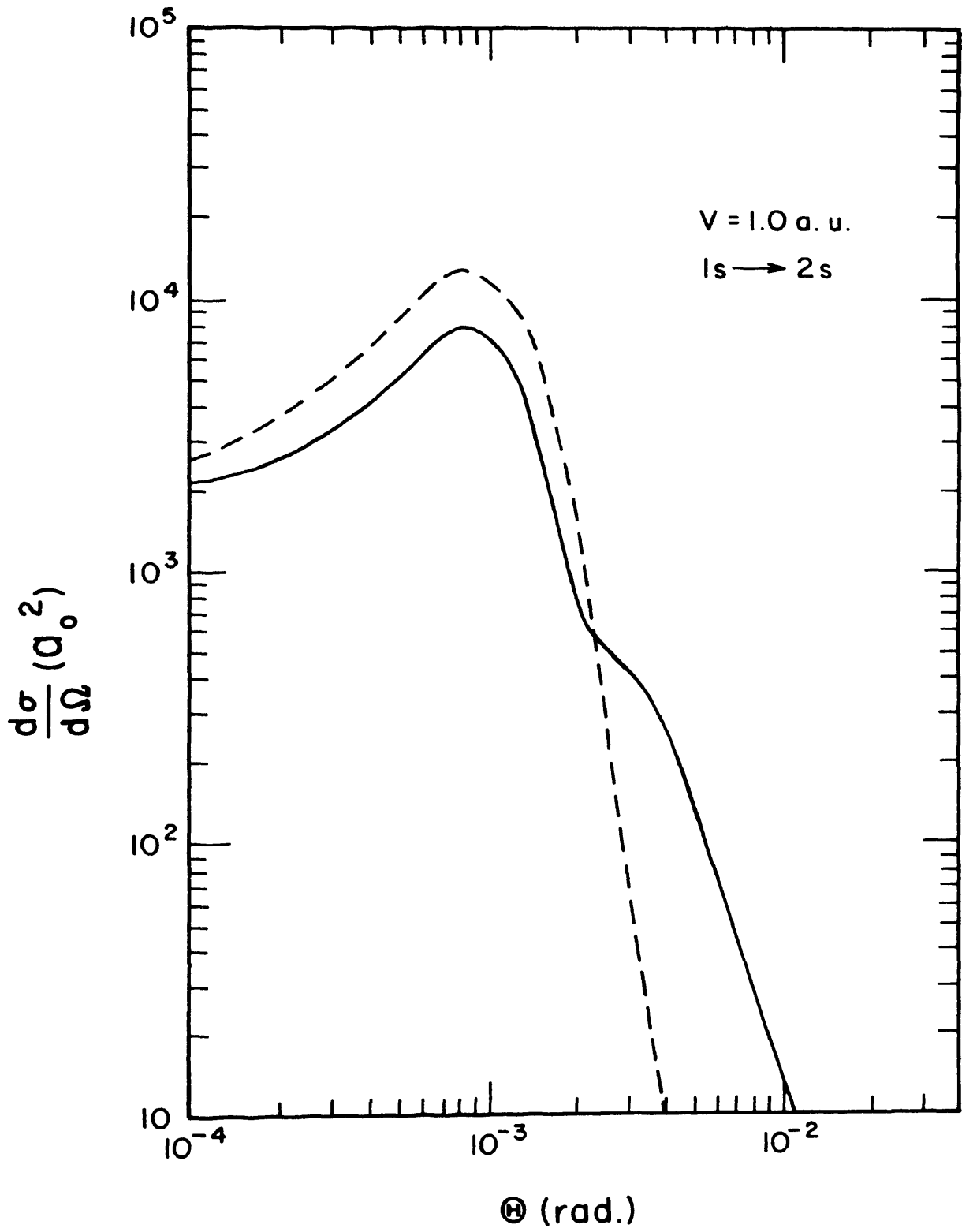angle are given in the center of mass coordinate system.

$$\frac{d\sigma}{d\Omega} \, (a_o^2)$$

V = .3 a. u.

Is ⟶ 2p₀

Is ⟶ 2p₊

Θ (rad.)

Figure 6

FIG. 7. Differential cross section for the excitation of hydrogen to the $2p_0$ and $2p_+$ states by hydrogen impact for an incident velocity of 0.4 a.u. or for an incident energy of 4.0 keV. The solid line is the eikonal DWBA and the dashed line is the first Born approximation. Both the differential cross section and the scattering angle are given in the center of mass coordinate system.

$$\frac{d\sigma}{d\Omega} (a_o^2)$$

$V = .4 \, a.u.$

$Is \longrightarrow 2p_o$

$Is \longrightarrow 2p_+$

$\Theta \, (rad.)$

Figure 7

FIG. 8. Differential cross section for the excitation of

hydrogen to the $2p_0$ and $2p_+$ states by hydrogen impact for an incident

velocity of 0.5 a.u. or for an incident energy of 6.25 keV. The

solid line is the eikonal DWBA and the dashed line is the first Born

approximation. Both the differential cross section and the scattering

angle are given in the center of mass coordinate system.

Figure 8

FIG. 9. Differential cross section for the excitation of
hydrogen to the $2p_0$ and $2p_+$ states by hydrogen impact for an incident
velocity of 1.0 a.u. or for an incident energy of 25 keV. The solid
line is the eikonal DWBA and the dashed line is the first Born
approximation. Both the differential cross section and the
scattering angle are given in the center of mass coordinate system.

Figure 9

FIG. 10. Differential cross section for the excitation of hydrogen to the $2p_0$ and $2p_+$ states by hydrogen impact for an incident velocity of 2.0 a.u. or for an incident energy of 100 keV. The solid line is the eikonal DWBA and the dashed line is the first Born approximation. Both the differential cross section and the scattering angle are given in the center of mass coordinate system.
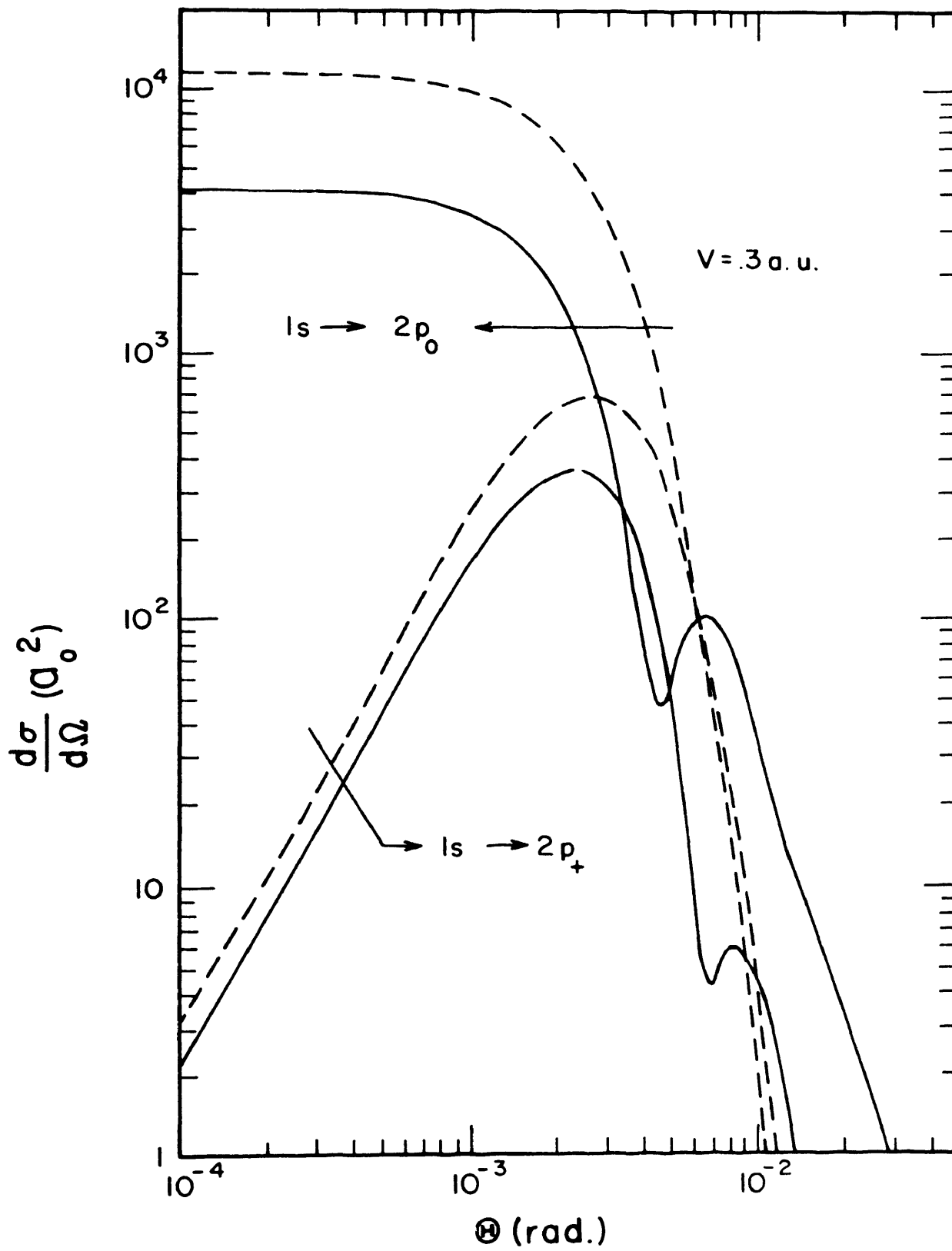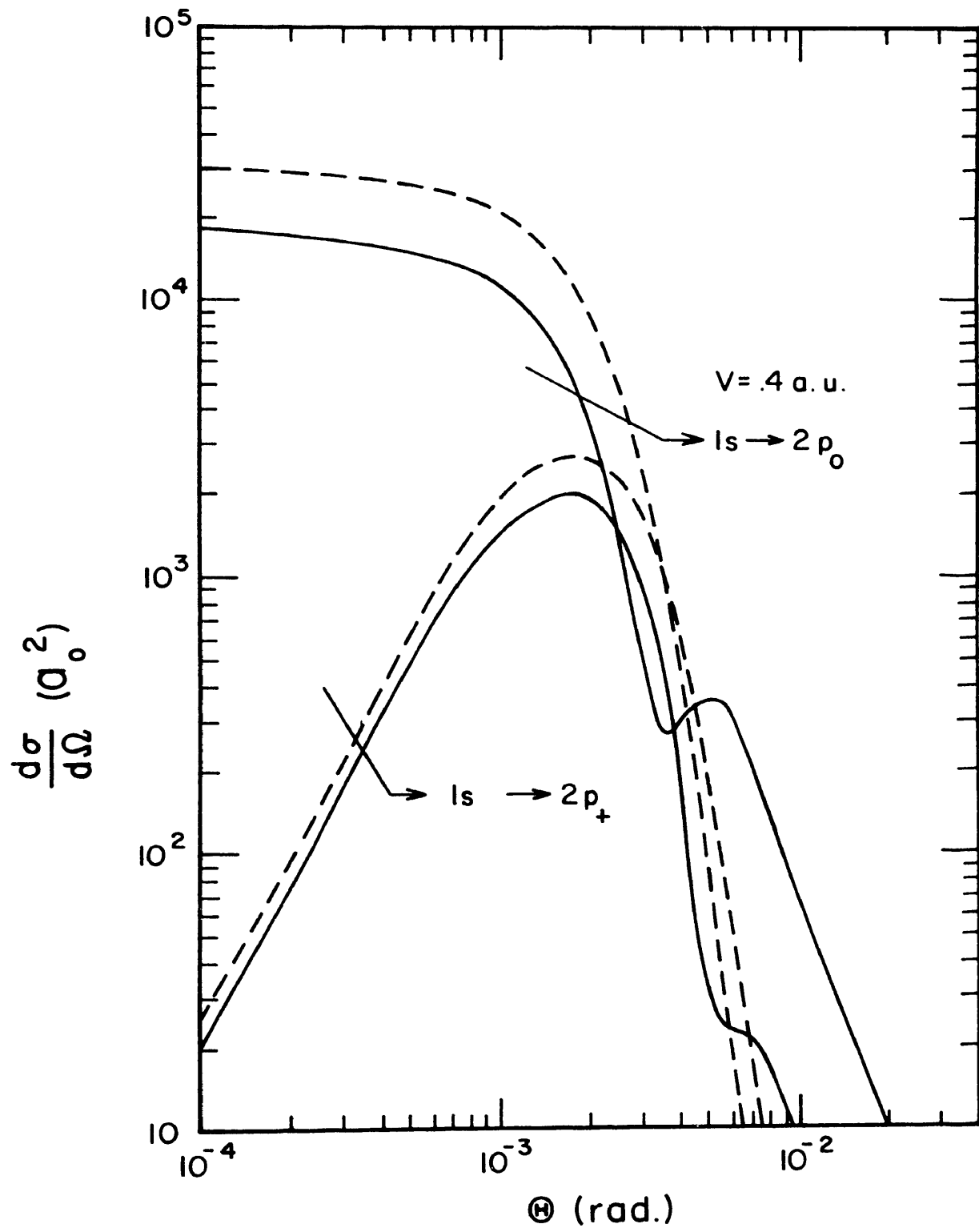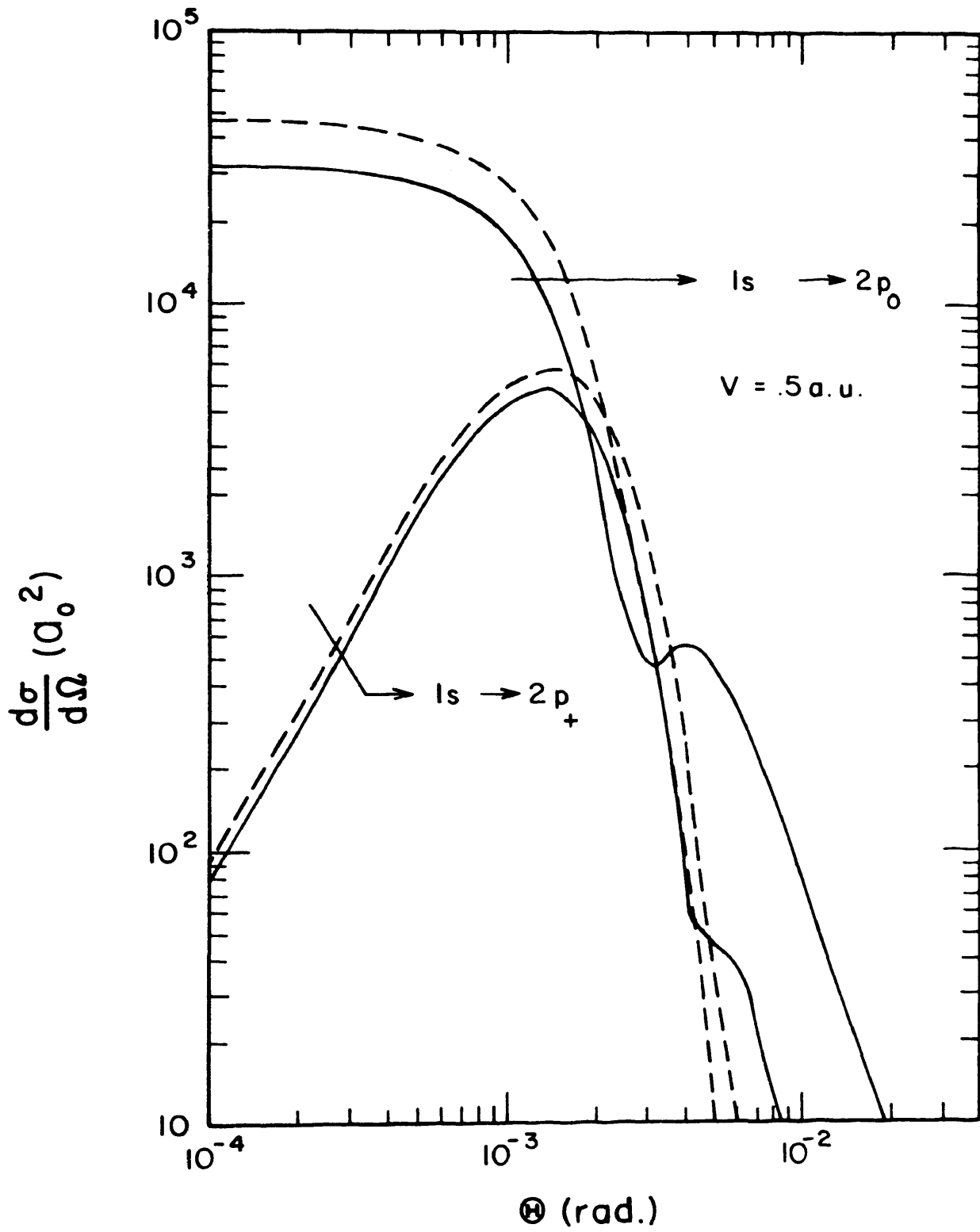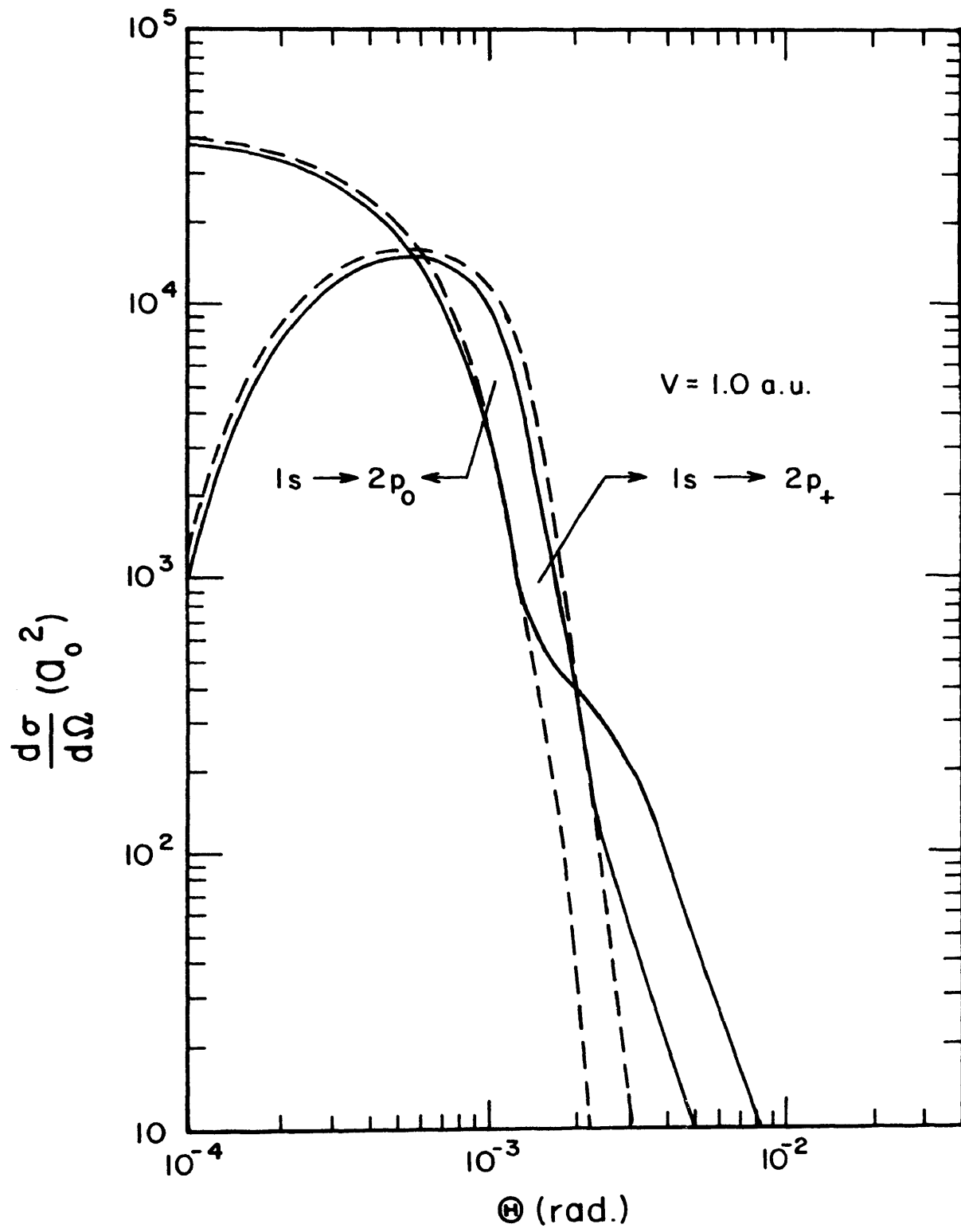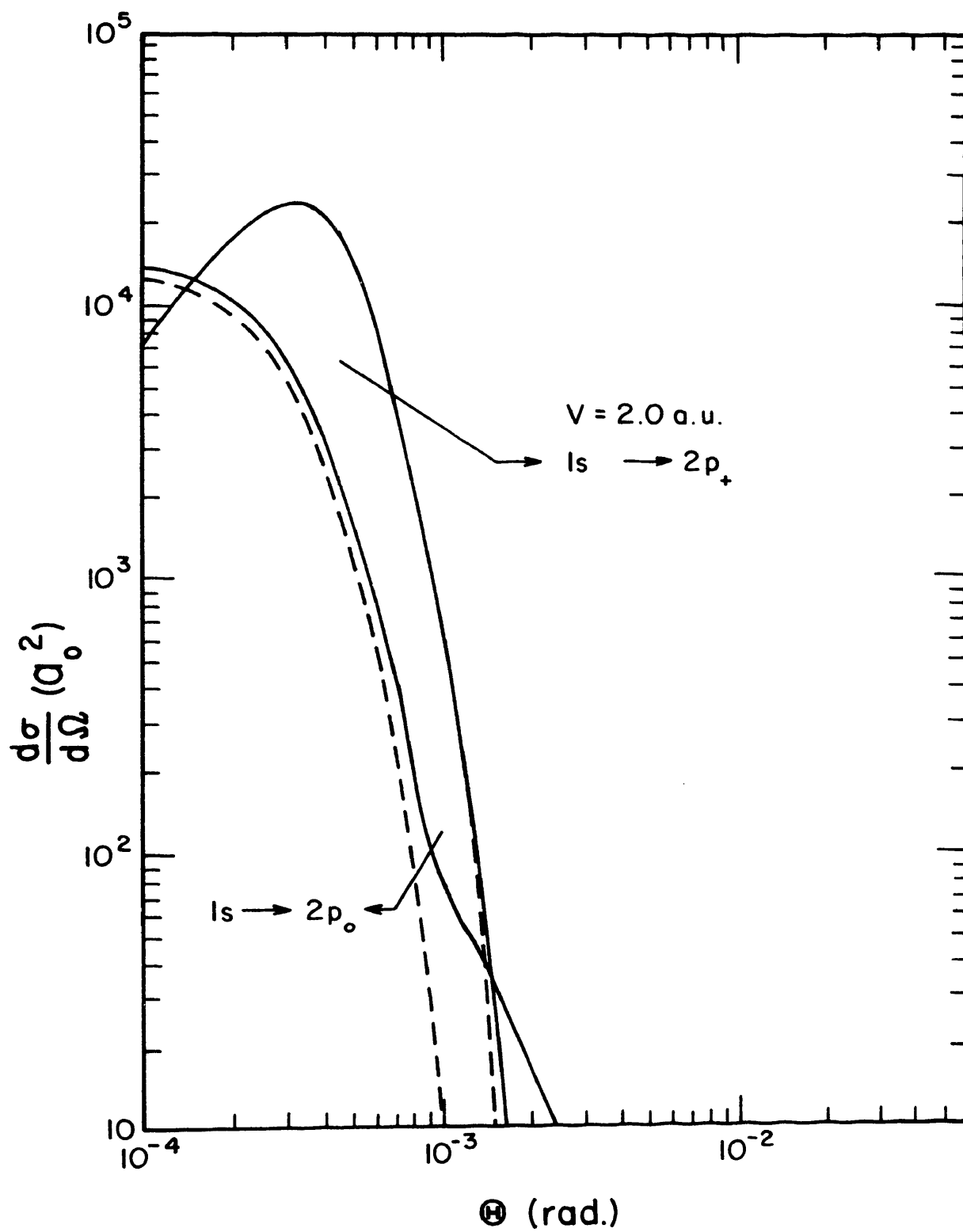
Figure 10

first Born approximation. The characteristics discussed for the 1s→2s excitation are still present. The eikonal DWBA curves are below the first Born approximation curves for small angles and then cross the Born curves and remain above them for the larger angles. This larger angle scattering is important in the calculation of the total cross section from the differential cross section. For the velocity $v = 1.0$ a.u., the eikonal differential cross section for the $2p_0$ excitation crosses the Born curve at a scattering angle of $\theta = 1.3 \times 10^{-3}$ rad. Twenty-three percent of the total cross section lies outside this crossing point. The $2p_+$ excitation differential cross section has a crossing point of $\theta = 2.2 \times 10^{-3}$ rad. at $v = 1.0$ a.u. and only 1% of the total cross section lies outside this region.

The second peak also occurs for the $2p_0$ and the $2p_+$ curves for the eikonal DWBA. These peaks become sharper at lower velocities as shown in Fig. 6 and then flatten out at higher velocities as shown in Figs. 7-10. The occurrence of these peaks is still attributed to the interference of the distortion factor $\exp[i \, \phi(b)]$ and the Bessel function $J_m(b \, k_f \sin\theta)$.

2. Total Cross Sections

The differential cross sections of the preceding section have been integrated to yield a total cross section. In Fig. 11, the total cross section for the 1s→2s excitation is presented for the eikonal DWBA, the first Born approximation, the 2- state and 4- state impact parameter calculation of Flannery[6], the impact parameter calculation

FIG. 11. Total cross section for the excitation of hydrogen to the 2s state by hydrogen impact. The solid line is the eikonal DWBA and the dashed line is the first Born approximation. The dash-dot line (— · — ·) and the dotted line (· · · · ·) are the 4-state and the 2-state impact parameter calculations of Flannery, Ref. 6. The dash - double dot line (— ·· — ··) is the impact parameter calculation using symmetrized atomic orbitals by Bottcher and Flannery, Ref. 33, and the long dash line (——— ———) is the 2-state impact parameter calculation, including electron exchange and the translational motion of the electrons, by Ritchie, Ref. 34.
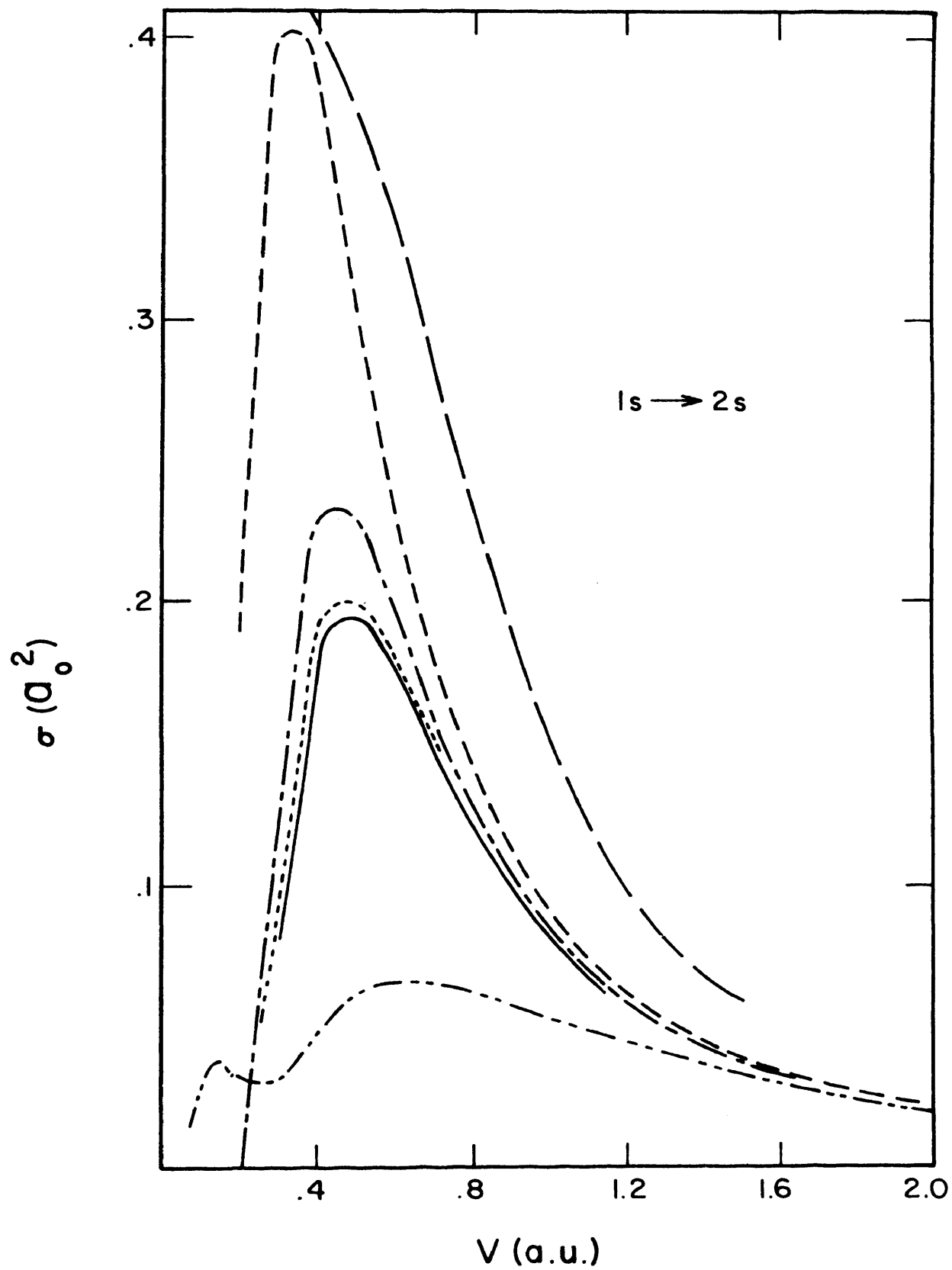
Figure 11

using symmetrized atomic orbitals by Bottcher and Flannery[33], and the 2-state impact parameter calculation including electron exchange and electron translational motion by Ritchie[34]. All the methods converge to the same curve for large velocities and differ considerably at the lower velocities. However, the eikonal DWBA does seem to follow the impact parameter calculations, especially the 2-state approximation.

In Figs. 12 and 13, the total cross sections are presented for the $2p_0$ and $2p_+$ excitation. The curves in these figures are the same as in Fig. 11 except the 2-state calculation of Flannery[6] has been deleted since it follows very close to the 4-state curve. Also the 2-state calculation of Ritchie[34] was only for the 2s excitation.

The closeness of the 2-state impact parameter method and the eikonal DWBA raises a question as to whether there is a relationship between the two methods. One can show that the eikonal DWBA can be reduced to the 2-state distortion approximation[35] in the limit of high energy and very small scattering angle, namely

$$|k_i| \gg (2M\Delta E)^{\frac{1}{2}} \tag{4.21}$$

and

$$\cos^{-1} \hat{k}_i \cdot \hat{k}_f = \theta \ll 1 \tag{4.22}$$

where ΔE is the change in kinetic energy or the electronic excitation energy. The conservation of energy equation can be approximated using Eq. (4.21) to obtain

$$k_i - k_f \simeq \Delta E/v \tag{4.23}$$

where $v \simeq v_i \simeq v_f$.

FIG. 12. Total cross section for the excitation of hydrogen to the $2p_0$ state by hydrogen impact. The solid line is the eikonal DWBA and the dashed line is the first Born approximation. The dash-dot line (— — — —) is the 4-state impact parameter calculation of Flannery, Ref. 6. The dash - double dot line (— — — — —) is the impact parameter calculation using symmetrized atomic orbitals by Bottcher and Flannery, Ref. 33.

$1s \longrightarrow 2p_0$

V(a.u.)
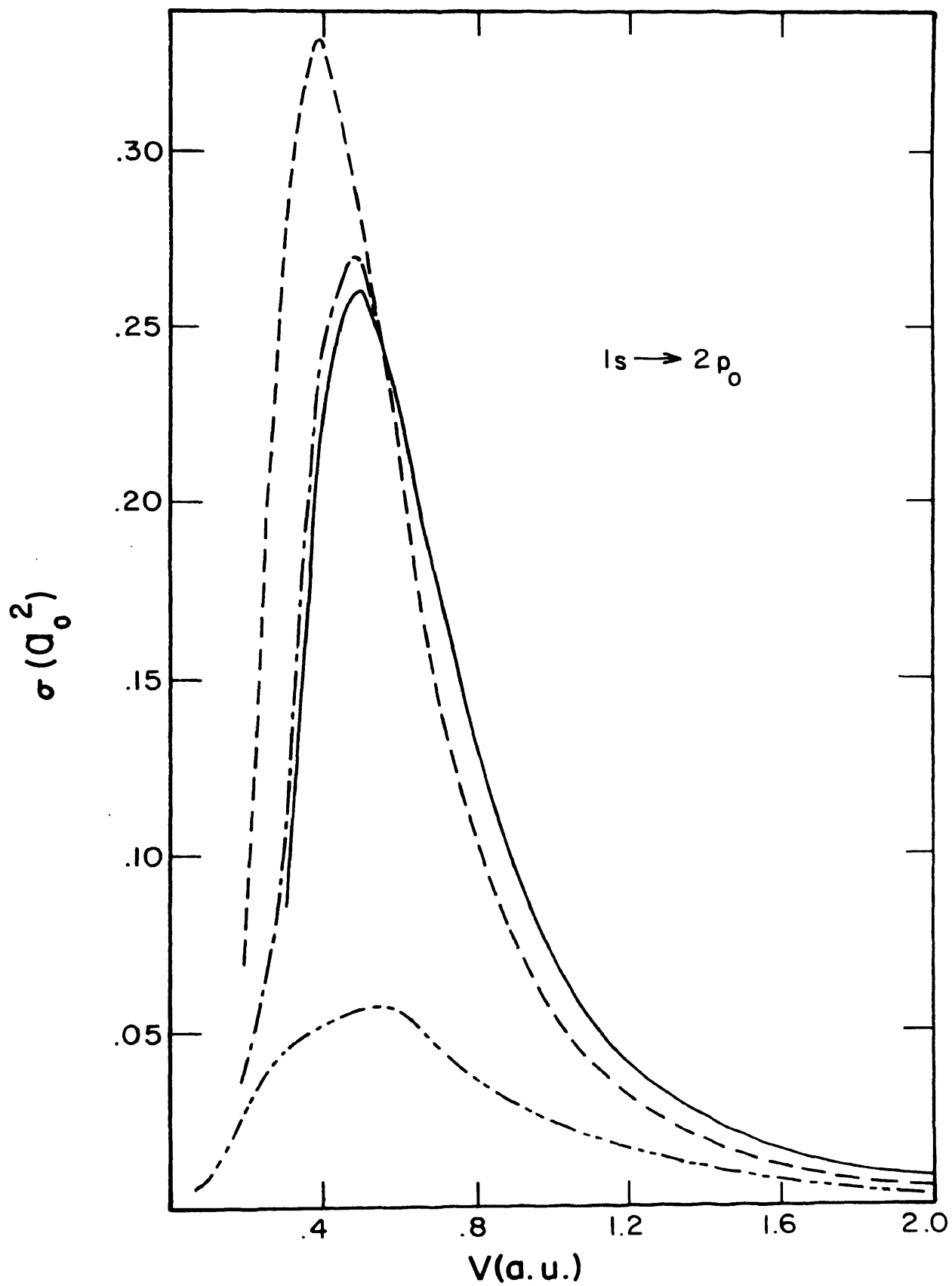
Figure 12

FIG. 13. Total cross section for the excitation of hydrogen to the $2p_+$ state by hydrogen impact. The solid line is the eikonal DWBA and the dashed line is the first Born approximation. The dash-dot line (— - — -) is the 4-state impact parameter calculation of Flannery, Ref. 6. The dash - double dot line (— -- — --) is the impact parameter calculation using symmetrized atomic orbitals by Bottcher and Flannery, Ref. 33.
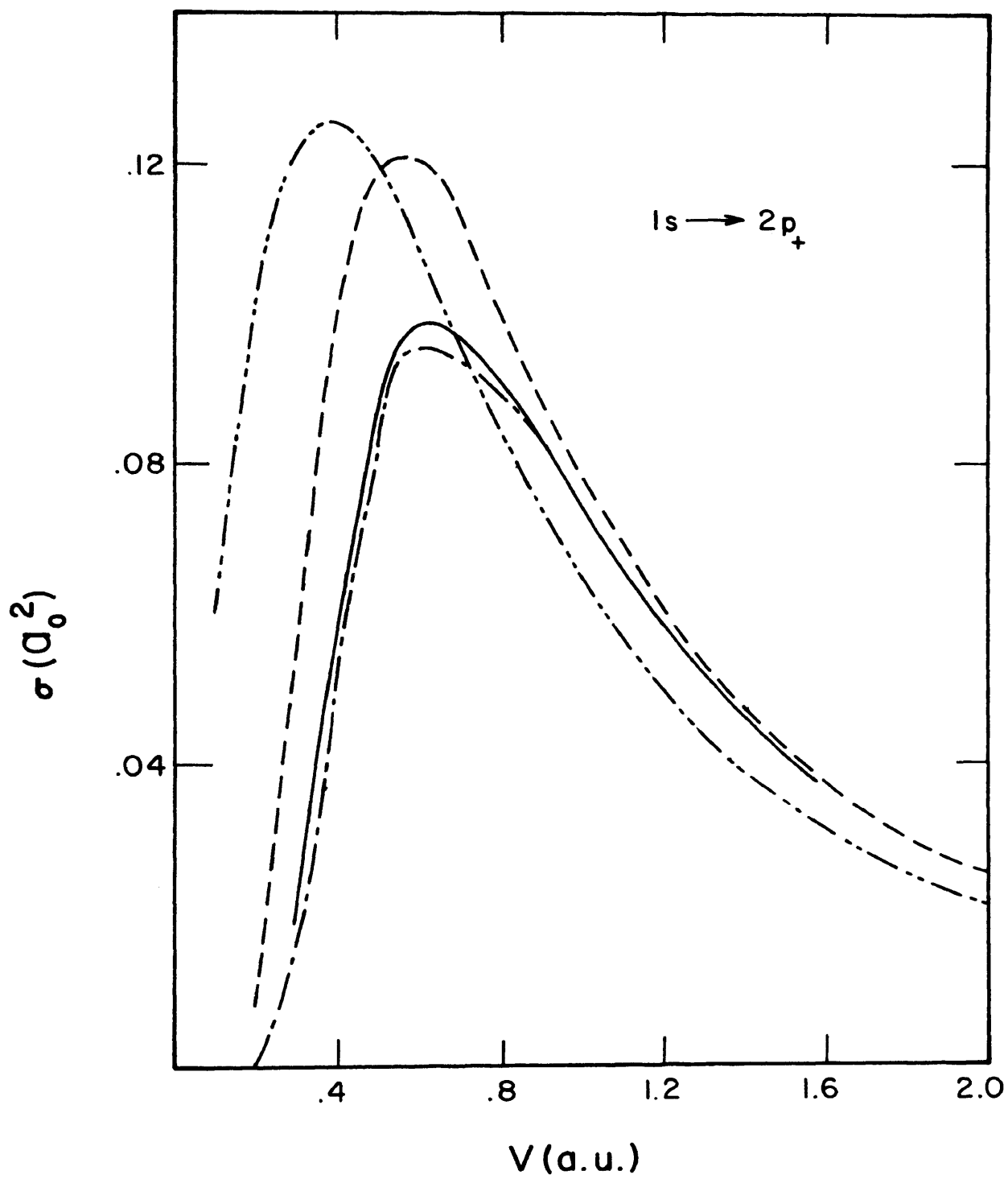
Figure 13

The T matrix, Eq. (3.39) can be written as

$$T_{fi}^{(eik)} = (2\pi)^{-3} \int_0^{2\pi} \int_0^{\infty} b \; db \; d\phi \int_{-\infty}^{\infty} dZ \; \exp[\frac{i \; \Delta E \; Z}{v} + i \; \delta \; \phi(b,Z)$$

$$+ i(\vec{k}_i - \vec{k}_f) \cdot \vec{b}] \; A(b,Z) \quad . \tag{4.25}$$

Using the notation introduced in Eqs. (4.13) and (4.14), the exponential factors can be written as

$$\frac{i \; \Delta E \; Z}{v} + i \; \delta \; \phi(b,Z) = i \; \phi(b) + \frac{i}{v} \; [\Delta E \; Z + \int_0^Z (U_f(b,Z') - U_i(b,Z'))dZ']$$

$$\equiv i \; \phi(b) + \frac{i}{v} \; N_{fi}(b,Z) \quad . \tag{4.26}$$

If U_i and U_f are taken to be the elastic matrix elements as given by Eqs. (4.2) and (4.3), then N_{fi} is the distortion factor for the transformed transition amplitude in the 2-state distortion approximation. The transition amplitude of Eq. (2.13) has been transformed by using

$$C_m(Z) = a_m(Z) \; \exp[\frac{i}{v} \int_0^Z U_m(b,Z')dZ'] \tag{4.27}$$

where $Z = vt$ has been used and the label m can be i or f. Eq. (2.14) can be rewritten then as

$$\frac{dC_m(Z)}{dZ} = \frac{1}{iv} \sum_{n=i}^{f} C_n(Z) \, V_{nm}(\vec{R}) \exp[-\frac{i}{v} N_{nm}] \tag{4.28}$$

where N_{nm} is defined by Eq. (4.26) and V_{nm} by Eq. (2.17). Also, it may be noted that $A(b,Z)$ of Eq. (4.8) and V_{nm} are just the off diagonal matrix elements. Eq. (4.28) can be solved in a two state approximation to give for the final state

$$C_f(b) = \frac{1}{v} \int_{-\infty}^{\infty} dZ \, A(b,Z) \exp[-\frac{i}{v} N_{if}] \ . \tag{4.29}$$

The T matrix (4.25) can be written using Eqs. (4.26), (4.29), and (2.24)

$$T_{fi}^{(eik)} = (2\pi)^{-3} \, v \int_{0}^{2\pi} \int_{0}^{\infty} b \, db \, d\phi \, e^{i\vec{q}\cdot\vec{b}} \, e^{i\phi(b)} \, C_f(b) \tag{4.30}$$

The total cross section then can be written as

$$\sigma_f = \int \frac{d\sigma}{d\Omega} \, d\Omega \tag{4.31}$$

Using the differential cross section, Eq. (3.15) and the transformation

$$d\Omega = \frac{d^2 q}{k_i \, k_f} \ , \tag{4.32}$$

the total cross section can be written as

$$\sigma_f = (2\pi)^{-2} \int \int d^2b \; d^2b' \; C_f(b) \; C_f^*(b') \; \exp[i\phi(b) - i\phi(b')]$$

$$\int_{q_{min}}^{q_{max}} d^2q \; e^{i\vec{q}\cdot(\vec{b}-\vec{b}')} \tag{4.33}$$

where

$$q_{min} = k_i - k_f \tag{4.34}$$

and

$$q_{max} = k_i + k_f \tag{4.35}$$

In the limit of high energy,

$$q_{min} \simeq 0 \tag{4.36}$$

and

$$q_{max} \simeq \infty \quad . \tag{4.37}$$

The q integration becomes a delta function for $\vec{b}$ and $\vec{b}'$. The cross section reduces to

$$\sigma_f = \int_0^\infty d^2b \, |C_f(b)|^2 \quad . \tag{4.38}$$

This shows that in the limits of the approximations mentioned the eikonal DWBA and the 2-state distortion approximation can be expected to yield similar results for the total cross section for very small angle scattering.

Electron exchange was neglected in this calculation. The problem involved with the inclusion of electron exchange in the eikonal DWBA will be discussed in section VI. Bottcher and Flannery[33] have performed a calculation to determine the effect of electron exchange. They used a multistate impact parameter approach. However, they included nuclear symmetry which is inconsistent with an impact parameter approach. Geltman[36] has pointed out that in any impact parameter method the assumption of a classical path forces the nuclei to be distinguishable. Thus Bottcher and Flannery[33] should not consider nuclear symmetry and their inclusion of it could be considered a source of error.

Bottcher and Flannery[33] took into account the rotation of the internuclear axis during the collision. They used a standard molecular integral program that uses molecular wave functions which are all quantized along the internuclear axis and then they transformed the results to a rotating frame.

The results of their calculation can be seen in Figs. 11-13. All of the cross sections are shifted from the results of Flannery's[6] impact parameter calculation. The peaks for the $1s \rightarrow 2s$ excitation cross sections and the $1s \rightarrow 2p_0$ excitation cross sections have been lowered considerably while the peak of the $1s \rightarrow 2p_+$ excitation cross sections has been shifted upwards. All the results tend to the Born cross sections at the higher velocities.

Bottcher and Flannery[33] did not include a phase factor to account for the translational motion of the electron. They argued that the neglected phase factors should become more important with

increasing energy. However, since their results tend to the Born cross sections at high energies, they concluded that the effect of the phase factor must be small.

Ritchie[34] has also performed a calculation to determine the effect of electron exchange. He assumed the nuclei were distinguishable for the reason mentioned above. However, he did not take into account the rotation of the internuclear axis during the collision. Instead he chose to include the translational motion of the electrons. The form of the unnormalized wave function he used was

$$\Psi_n = [\phi_{1s}(\vec{r}_{1A})\phi_n(\vec{r}_{2B})\ e^{-i\vec{v}'\cdot\vec{r}_1}\ e^{i\vec{v}'\cdot\vec{r}_2}$$

$$\pm\ \phi_{1s}(\vec{r}_{2A})\phi_n(\vec{r}_{1B})\ e^{i\vec{v}'\cdot\vec{r}_1}\ e^{-i\vec{v}'\cdot\vec{r}_2}] \qquad (4.39)$$

where r_1 and r_2 are the distances from the center of mass to electrons 1 and 2, respectively, and v' is one half the relative velocity. The plus or minus is taken depending upon whether the spin state of the electrons is a singlet or a triplet. The phase factors are included to account for the translational motion of the electrons.

The resulting cross section can be seen in Fig. 11. The results of Ritchie[34] and the results of Bottcher and Flannery[33] show a large disagreement at all velocities. The peaks are separated by a factor of eleven. This large discrepancy between the theoretical results raises some questions on how electron exchange should be included.

Ritchie[37] in the calculation of the matrix elements makes the assumption that the velocity of the projectile is along the

internuclear axis. That is, the matrix elements were calculated for a head on collision. This greatly simplified the calculation of the matrix elements, but he assumes that the matrix elements that were calculated for a head on collision can now be used in a 2-state impact parameter calculation in which the projectile remains at a constant impact parameter from the Z axis during the collision. His assumption that the velocity is along the internuclear axis does not allow for the rotation of the internuclear axis during the collision and would be a source of error.

The matrix elements are a double sum due to the expansions of the plane wave $\exp(i\vec{v}'\cdot\vec{r}_1)$ and the electron-electron interaction term $1/|\vec{r}_1-\vec{r}_2|$. The restriction that the velocity is along the internuclear axis enables the double sum to be reduced to a single sum. However, Ritchie's[34] assumption that the relative velocity is along the internuclear axis is unphysical since the relative velocity decreases as the impact parameter becomes larger. If one uses a molecular state basis, the rotation of the internuclear axis must be considered.

The divergent results of the two methods still raises doubts as to the importance of electron exchange in the intermediate energy range and also how electron exchange should be included since both approaches contain unphysical assumptions.

V. EXCITATION OF HYDROGEN TO THE 2s AND 2p STATES BY HELIUM IMPACT

A. Basic Equations

The eikonal DWBA has been applied to the H-He collisions given by Eq. (1.1) in the energy range of 2.25 keV (v = .3 a.u.) to 100 keV (v = 2.0 a.u.).

The interaction potential was taken as

$$V(\vec{R},\vec{r}_A,\vec{r}_B) = \frac{2}{R} + \sum_{i=1}^{2} \frac{1}{|\vec{R}+\vec{r}_{iA}-\vec{r}_B|} - \sum_{i=1}^{2} \frac{1}{|\vec{R}+\vec{r}_{iA}|} - \frac{2}{|\vec{R}-\vec{r}_B|} \quad (5.1)$$

where r_A and r_B are electronic coordinates for the He and H atoms, respectively.

The wave function of the ground state helium atom needed in the calculation was taken as the following Hartree-Fock function[38].

$$\phi_{1's}(\vec{r}_A) = \frac{1.6966}{\pi} (e^{-1.4r_{1A}} + .799\ e^{-2.61r_{1A}})$$

$$(e^{-1.4r_{2A}} + .799\ e^{-2.61r_{2A}}) \quad (5.2)$$

The optical potentials are represented by the static matrix elements. That is

$$U_i = <\phi_{1's}(\vec{r}_A)\phi_{1s}(\vec{r}_B)|V(\vec{R},\vec{r}_A,\vec{r}_B)|\phi_{1's}(\vec{r}_A)\phi_{1s}(\vec{r}_B)>$$

$$= e^{-2.82R}(-.0414 - \frac{5.02}{R}) + e^{-4.02R}(1.20 + \frac{.403}{R})$$

$$+ e^{-5.22R}(.309 + \frac{.110}{R}) + e^{-2R}(-4.25 + \frac{6.50}{R}) \quad (5.3)$$

Likewise,

$$U_f^{2s} = e^{-R}(-.0592\ R^2 + .306\ R - .540 + \frac{.319}{R})$$

$$+ e^{-2.82\ R}\ (1.60 + \frac{.917}{R}) + e^{-4.02\ R}\ (1.33 + \frac{.642}{R})$$

$$+ e^{-5.22\ R}\ (.317 + \frac{.121}{R})\quad . \tag{5.4}$$

Also

$$U_f^{2p_o} = U_0(R) - \sqrt{\frac{5}{4\pi}}\ (\frac{3Z^2}{R^2} - 1)\ U_2(R) \tag{5.5}$$

and

$$U_f^{2p_+} = U_0(R) + \frac{1}{2}\ \sqrt{\frac{5}{4\pi}}\ (\frac{3Z^2}{R^2} - 1)\ U_2(R) \tag{5.6}$$

where

$$U_0(R) = e^{-2.82\ R}\ (1.70 + \frac{1.19}{R}) + e^{-4.02\ R}\ (1.34 + \frac{.667}{R})$$

$$+ e^{-5.22\ R}\ (.318 + \frac{.121}{R}) + e^{-R} \times 10^{-2}\ (-1.98\ R^2$$

$$+ 2.29\ R - 3.99 + \frac{2.27}{R}) \tag{5.7}$$

and

$$U_2(R) = e^{-2.82\ R} \times 10^{-2}\ (1.84 + \frac{7.94}{R} + \frac{7.75}{R^2} + \frac{2.75}{R^3})$$

$$+ e^{-4.02\ R} \times 10^{-3}\ (1.30 + \frac{3.73}{R} + \frac{2.54}{R^2} + \frac{.633}{R^3})$$

$$+ e^{-5.22\ R} \times 10^{-4}\ (.579 + \frac{1.25}{R} + \frac{.656}{R^2} + \frac{.126}{R^3})$$

$$+ e^{-R} \times 10^{-2}(3.13\ R^2 - 3.65\ R + 2.66 + \frac{1.73}{R} - \frac{2.81}{R^2} - \frac{2.81}{R^3})\quad . \tag{5.8}$$

The off diagonal matrix elements are given by

$$A_{2s}(\vec{R}) = <\phi_{1's}(\vec{r}_A)\phi_{2s}(\vec{r}_B)|V(\vec{R},\vec{r}_A,\vec{r}_B)|\phi_{1's}(\vec{r}_A)\phi_{1s}(\vec{r}_B)>$$

$$= e^{-1.5 R}(.442 R - 1.53 + \frac{1.31}{R}) - e^{-2.82 R}(.414R + \frac{1.23}{R})$$

$$- e^{-4.02 R} \times 10^{-2}(4.56 + \frac{7.90}{R})$$

$$- e^{-5.22 R} \times 10^{-3}(3.14 + \frac{3.93}{R}) \quad . \tag{5.9}$$

Likewise,

$$A_{2p_0}(\vec{R}) = \sqrt{\frac{3}{4\pi}} \; \frac{Z}{R} A_0(R) \tag{5.10}$$

and

$$A_{2p_+}(\vec{R}) = -\sqrt{\frac{3}{8\pi}} \; \frac{b}{R} e^{i\phi} A_0 \tag{5.11}$$

where

$$A_0(R) = e^{-2.82 R}(.451 + \frac{1.61}{R} + \frac{.588}{R^2})$$

$$+ e^{-4.02 R} \times 10^{-2}(3.48 + \frac{7.77}{R} + \frac{1.93}{R^2})$$

$$+ e^{-5.22 R} \times 10^{-3}(1.85 + \frac{3.02}{R} + \frac{.578}{R^2})$$

$$+ e^{-1.5 R}(-.901 R + 1.33 - \frac{.911}{R} - \frac{.608}{R^2}) \quad . \tag{5.12}$$

The T matrix, Eq. (3.39), can be simplified by using the same procedures as was used for the H-H collision T matrix elements.

Eqs. (4.12) to (4.20) would be applicable by simply substituting the H-He matrix elements in for the H-H matrix elements.

B. Results and Discussion

1. Differential Cross Sections

The differential cross sections for the 1s→2s excitation are presented in Figs. 14-17 for the incident velocities v = .3, .632, 1.0, and 2.0 a.u. The eikonal DWBA results are compared to the first Born approximation results and in Fig. 15 to the experiment of Sauers, Nichols, and Thomas[12].

The eikonal DWBA results have the same characteristics for the H-He collisions as they did for the H-H collisions results presented in section IV. The differential cross sections for the eikonal DWBA lie below the Born results for small angles and remain above them for larger angles. A significant amount of the total cross section is scattered into the larger angle region.

The second peak is also present in the eikonal DWBA results. The peak is quite sharp for low velocities, Fig. 14, and dies out for high velocities, Fig. 17. The occurrence of this peak is attributed to the interference of the distortion factor $\exp[i\ \phi(b)]$ and the term $J_m(k_f b\sin\theta)$.

A direct comparison of the H-H results and the H-He results (for example, Fig. 4 to Fig. 16) in the center of mass frame shows that the H-He results peak at a higher value and at a smaller angle. Also, the second peak in the H-He results occur at a higher value and at a smaller angle in comparison to the H-H results. However,

FIG. 14. Differential cross sections for the excitation of
hydrogen to the 2s state by helium impact for an incident velocity
of 0.3 a.u. or for an incident energy of 2.25 keV. The solid line
is the eikonal DWBA and the dashed line is the first Born approxima-
tion. Both the differential cross section and the scattering angle
are given in the center of mass coordinate system.

Figure 14

FIG. 15. Differential cross sections for the excitation of hydrogen to the 2s state by helium impact for an incident velocity of 0.6324 a.u. or for an incident energy of 10 keV. The solid line is the eikonal DWBA and the dashed line is the first Born approximation. The circles are the experimental data of Sauers, Nichols and Thomas, Ref. 12, and have been multiplied by a factor of four. Both the differential cross section and the scattering angle are given in the center of mass coordinate system.

V = .6324 a.u.

E = 10 keV

1s ⟶ 2s

$\frac{d\sigma}{d\Omega}$ (a_o^2)

Θ (rad.)

Figure 15

FIG. 16. Differential cross sections for the excitation of
hydrogen to the 2s state by helium impact for an incident velocity
of 1.0 a.u. or for an incident energy of 25 keV. The solid line is
the eikonal DWBA and the dashed line is the first Born approximation.
Both the differential cross section and the scattering angle are
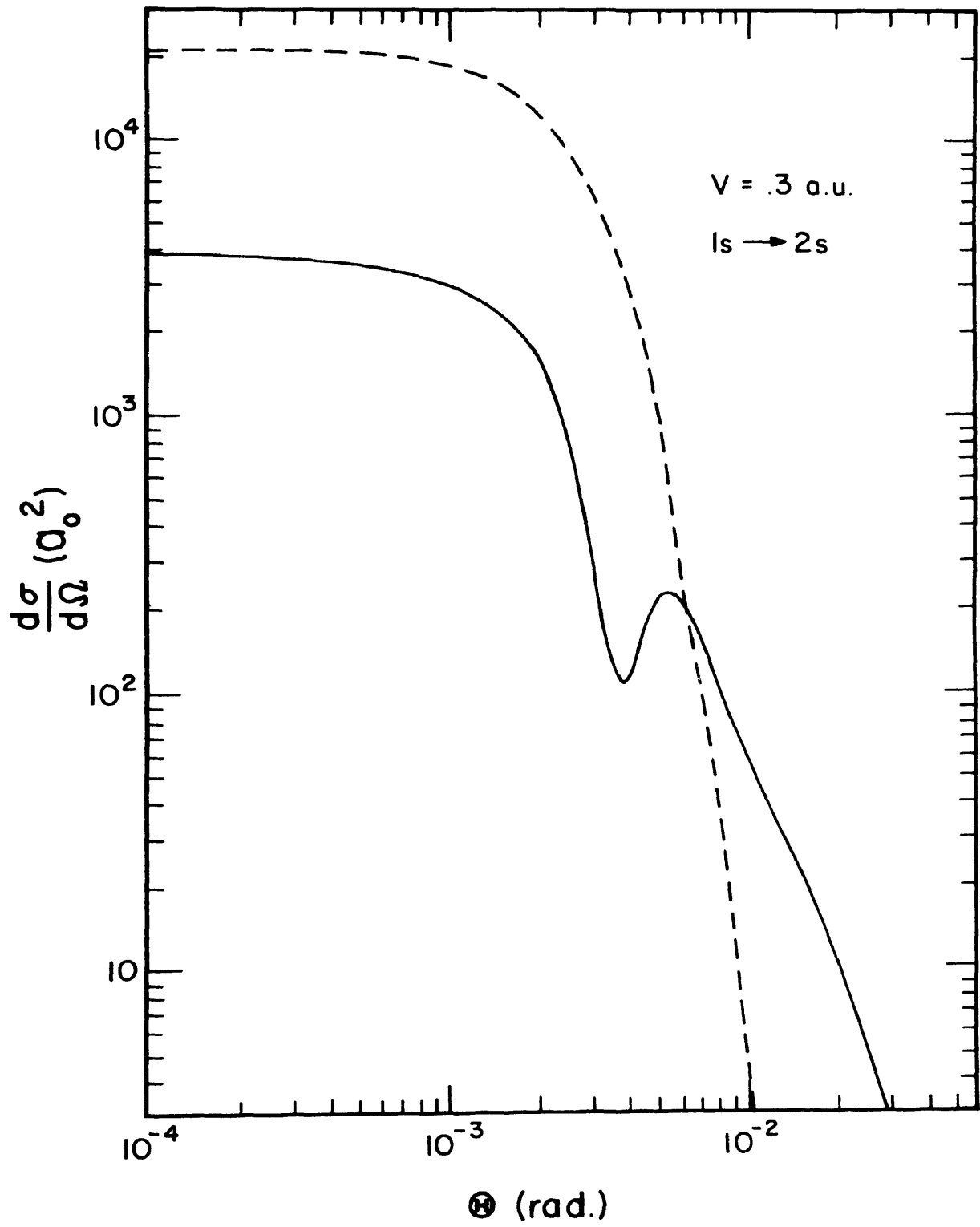given in the center of mass coordinate system.

$V = 1.0$ a.u.

$ls \longrightarrow 2s$

$\frac{d\sigma}{d\Omega}$ (a_o^2)

Θ (rad.)

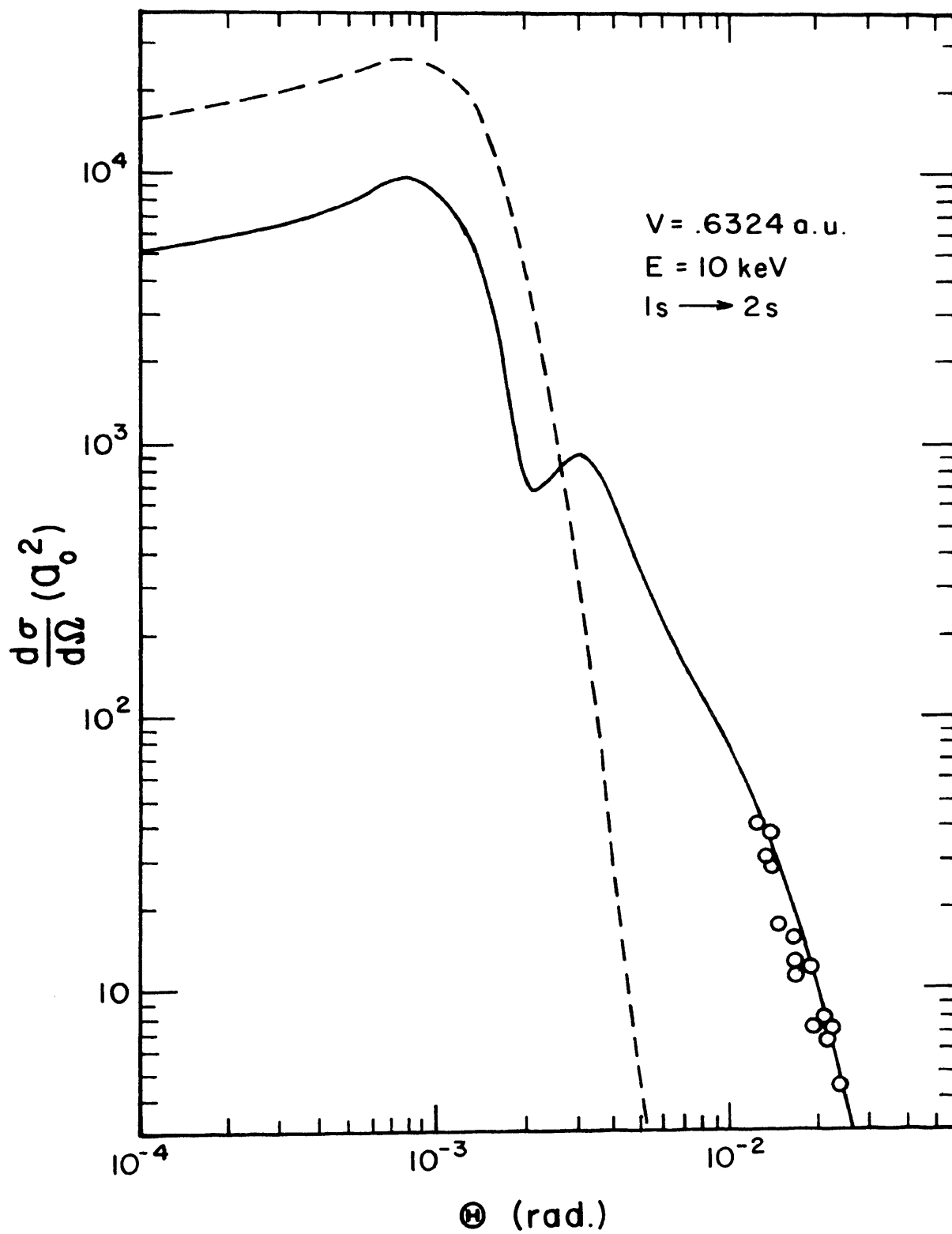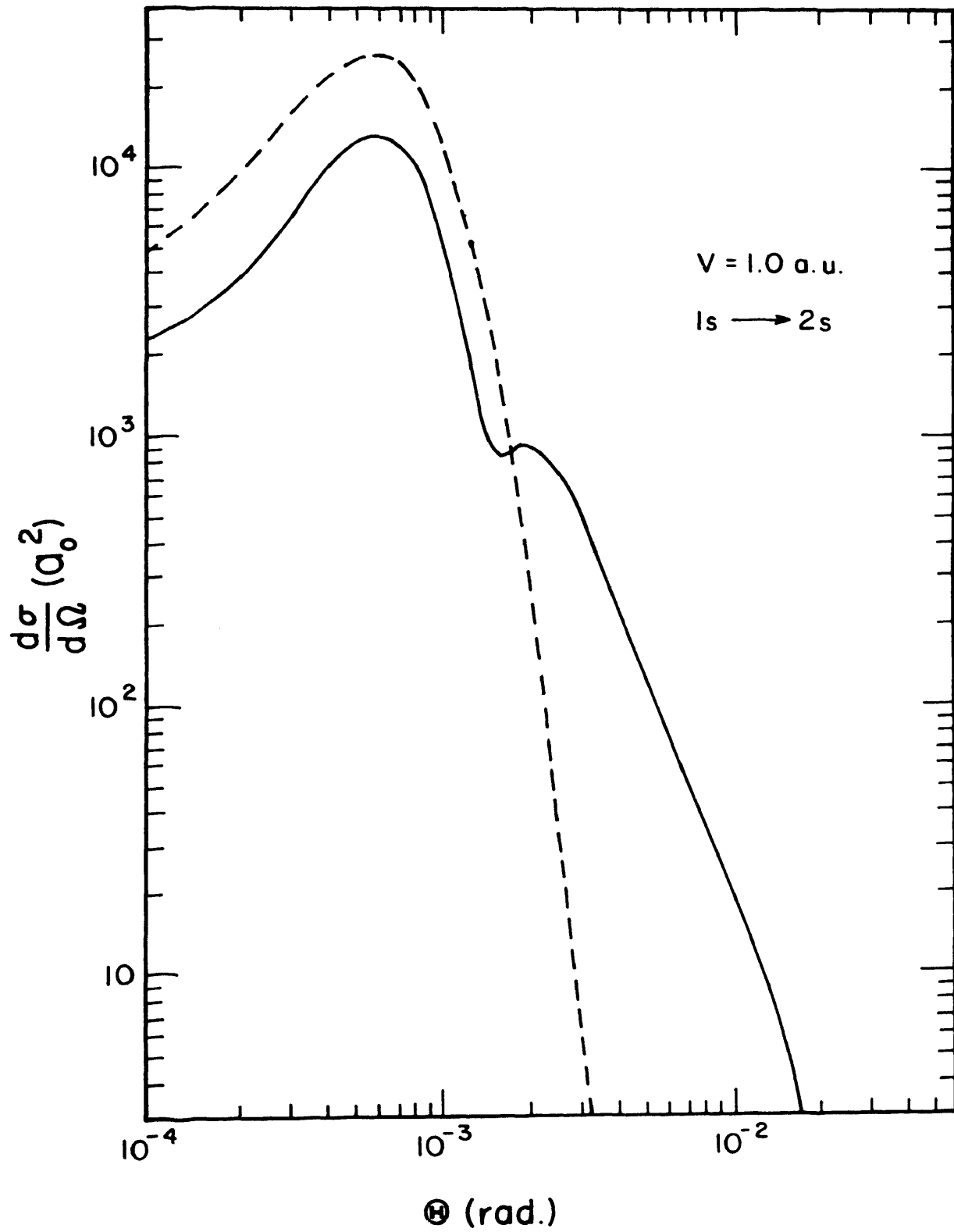Figure 16

FIG. 17. Differential cross sections for the excitation of hydrogen to the 2s state by helium impact for an incident velocity of 2.0 a.u. or for an incident energy of 100 keV. The solid line is the eikonal DWBA and the dashed line is the first Born approximation. Both the differential cross section and the scattering angle are given in the center of mass coordinate system.
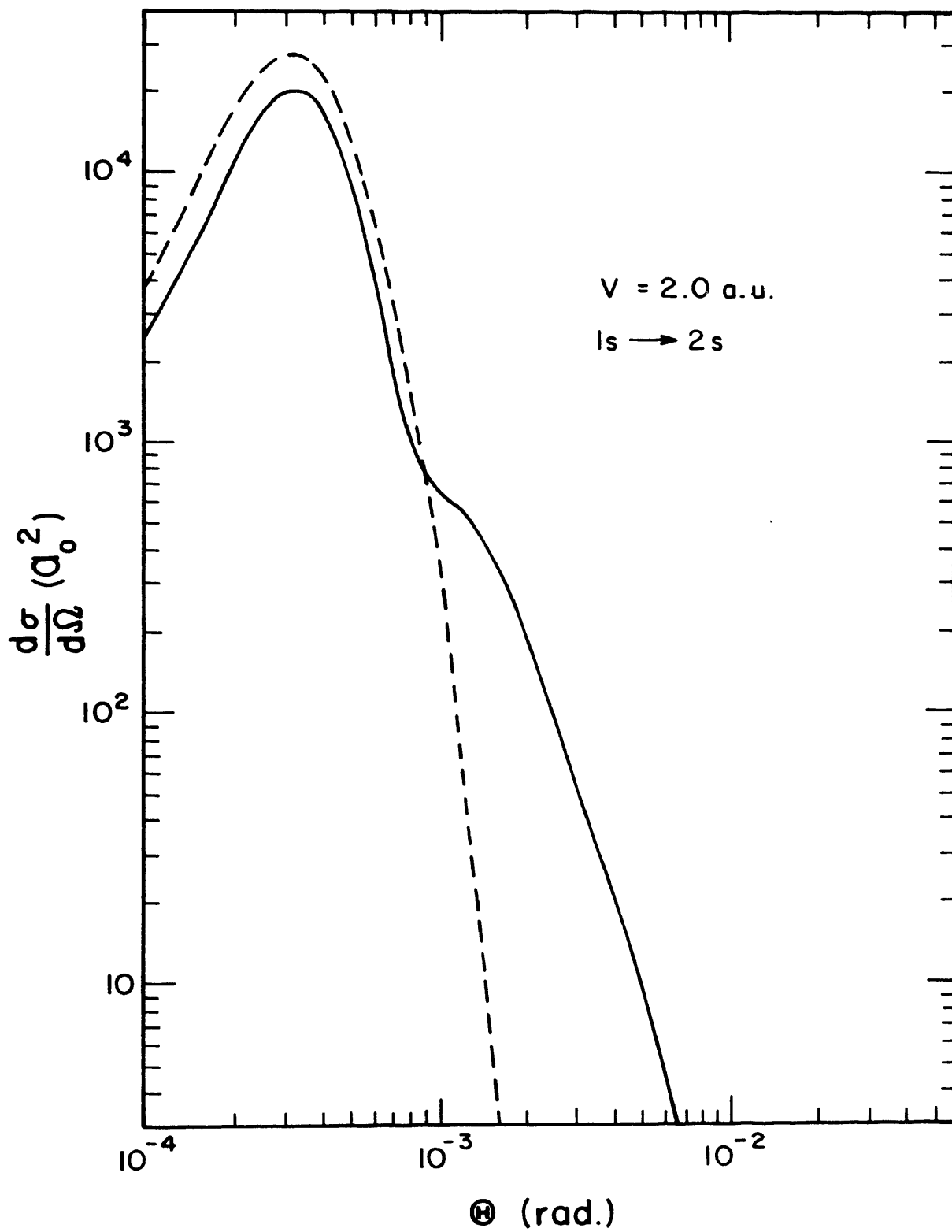
Figure 17

if both results are transformed to the laboratory frame, a comparison of the results show that most of the differences can be attributed to the difference in the reduced masses of the H-H and H-He systems. In the laboratory frame, the H-H results lie above the H-He results for small angles and then lie slightly below for large angles. The first and second peaks for both collisions occur at the same angle.

In Fig. 15, a comparison is made to the experimental data of Sauers, Nichols, and Thomas[12]. Their results have been multiplied by a factor of four. The comparison shows good agreement for both the shape and the slope of the curves. The experiment shows that large angle scattering does occur and that it is dying off slowly. The relative magnitude being off by such large factor is an unresolved problem. The experimental data at the time of this writing is unpublished, so the details of the actual experiment are unknown. The procedure that Sauers, et al.[12] used to normalize the experimental data could possibly account for the constant factor between the theoretical and experimental results. It would be of interest to know if the differential cross section of Sauers, et al.[12], could be integrated to give the total cross section of previously published results. If the total cross section disagrees by a constant factor, then a systematic error in the experimental results of Sauers, et al.[12], would be indicated. However, at this time only conjectures can be made.

A similar set of results are presented in Figs. 18-21 for the $2p_o$ and the $2p_+$ excitations for the incident velocities $v = .3, .5,$ 1.0, and 2.0 a.u. The same general comments mentioned before also

FIG. 18. Differential cross section for the excitation of hydrogen to the $2p_0$ and $2p_+$ states by helium impact for an incident velocity of 0.3 a.u. or for an incident energy of 2.25 keV. The solid line is the eikonal DWBA and the dashed line is the first Born approximation. Both the differential cross section and the scattering angle are given in the center of mass coordinate system.

$1s \longrightarrow 2p_o$

$V = .3$ a.u.

$1s \longrightarrow 2p_+$

$\dfrac{d\sigma}{d\Omega} (a_o^2)$

Θ (rad.)

Figure 18

FIG. 19. Differential cross section for the excitation of hydrogen to the $2p_0$ and $2p_+$ states by helium impact for an incident velocity of 0.5 a.u. or for an incident energy of 6.25 keV. The solid line is the eikonal DWBA and the dashed line is the first Born approximation. Both the differential cross section and the scattering angle are given in the center of mass coordinate system.

Figure 19

FIG. 20. Differential cross section for the excitation of hydrogen to the $2p_0$ and $2p_+$ states by helium impact for an incident velocity of 1.0 a.u. or for an incident energy of 25 keV. The solid line is the eikonal DWBA and the dashed line is the first Born approximation. Both the differential cross section and the scattering angle are given in the center of mass coordinate system.

Figure 20

FIG. 21. Differential cross section for the excitation of hydrogen to the $2p_0$ and $2p_+$ states by helium impact for an incident velocity of 2.0 a.u. or for an incident energy of 100 keV. The solid line is the eikonal DWBA and the dashed line is the first Born approximation. Both the differential cross section and the scattering angle are given in the center of mass coordinate system.
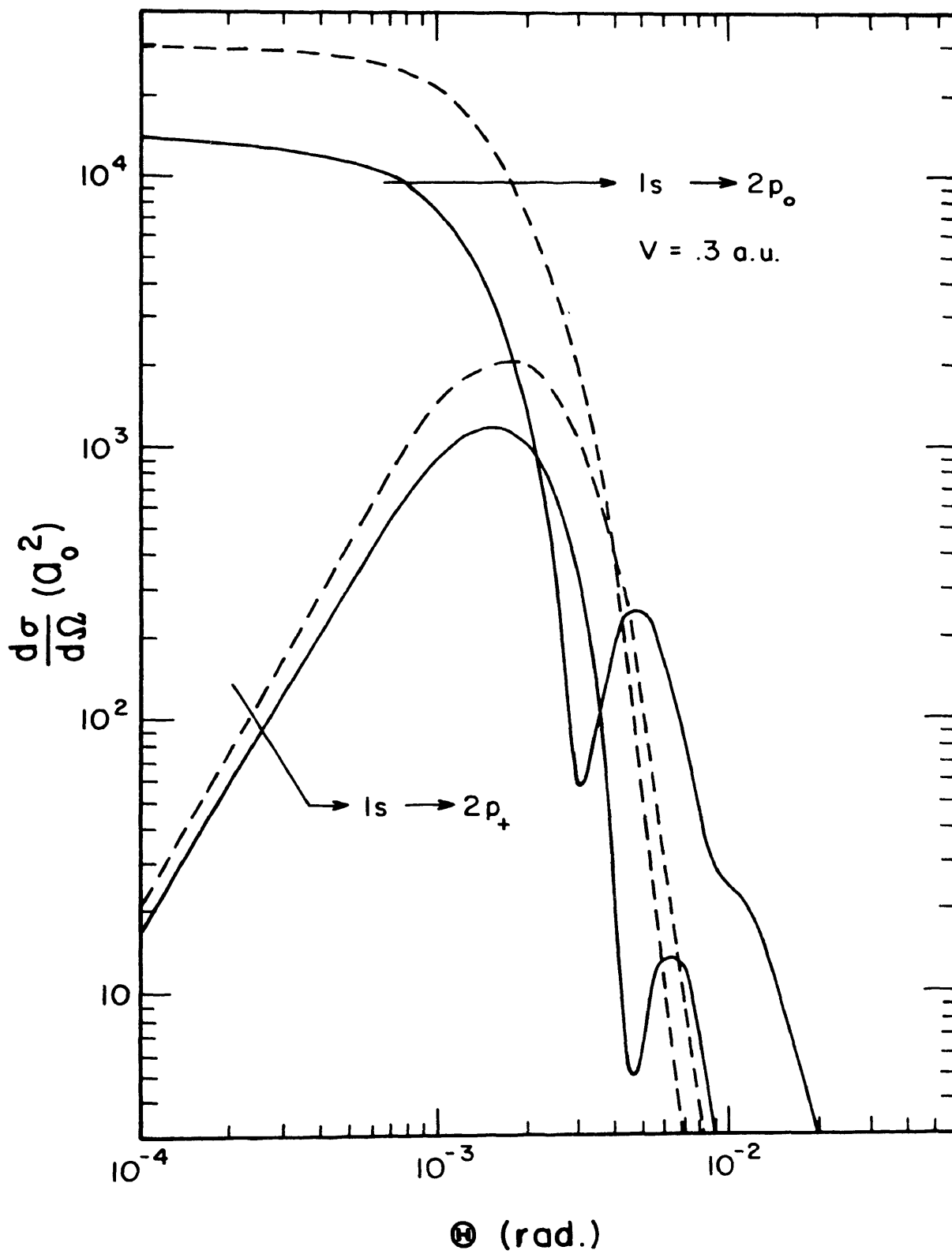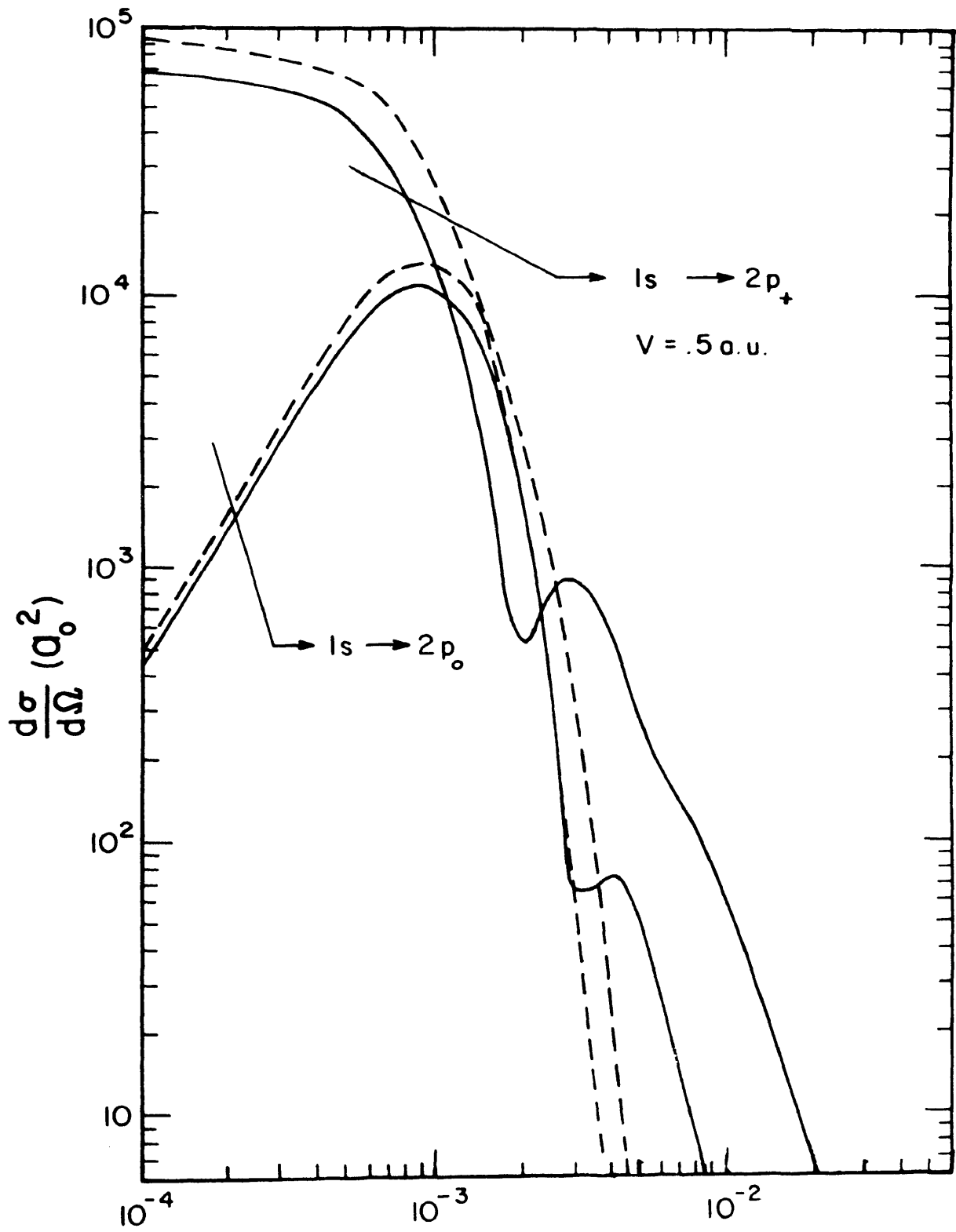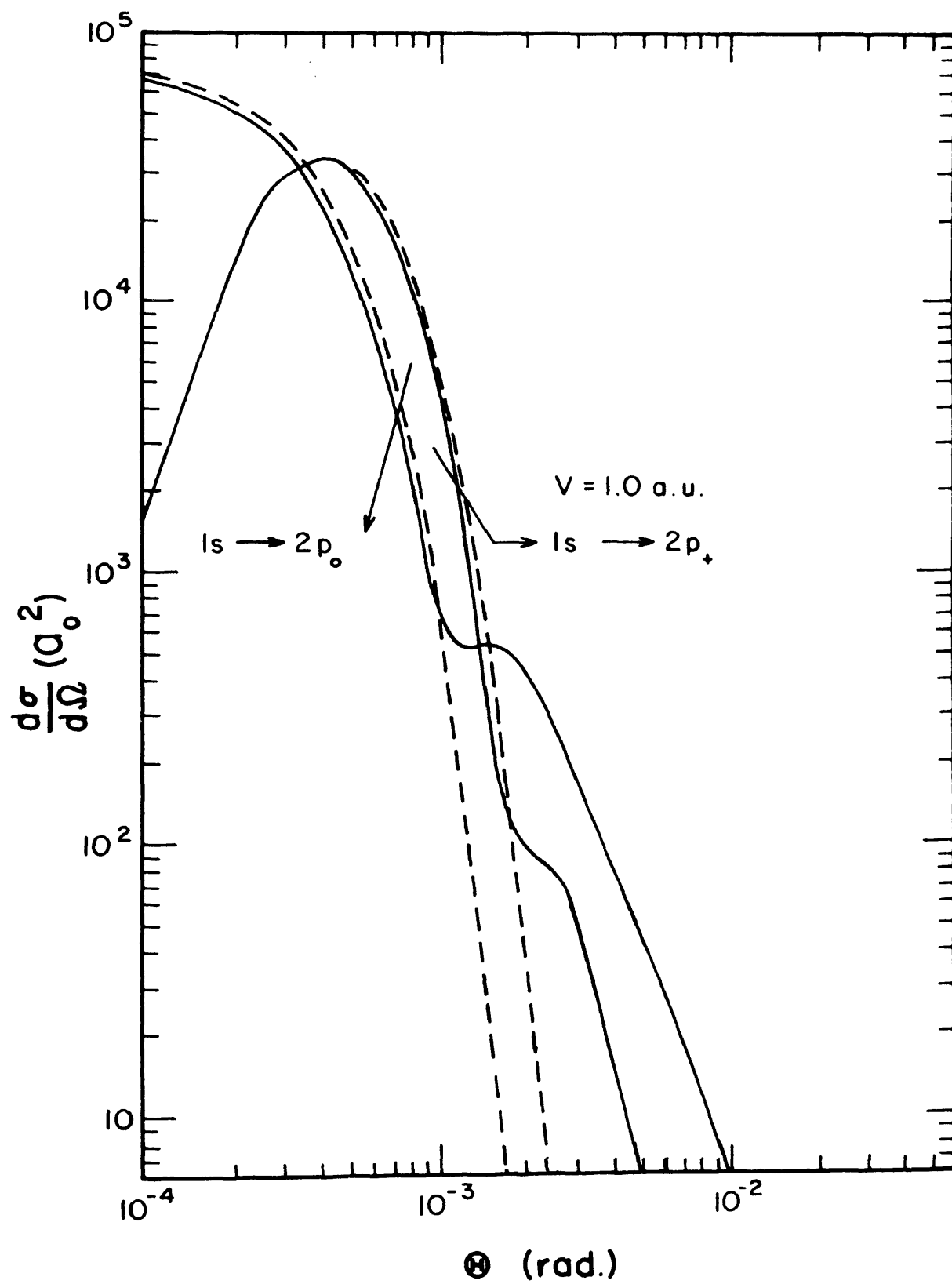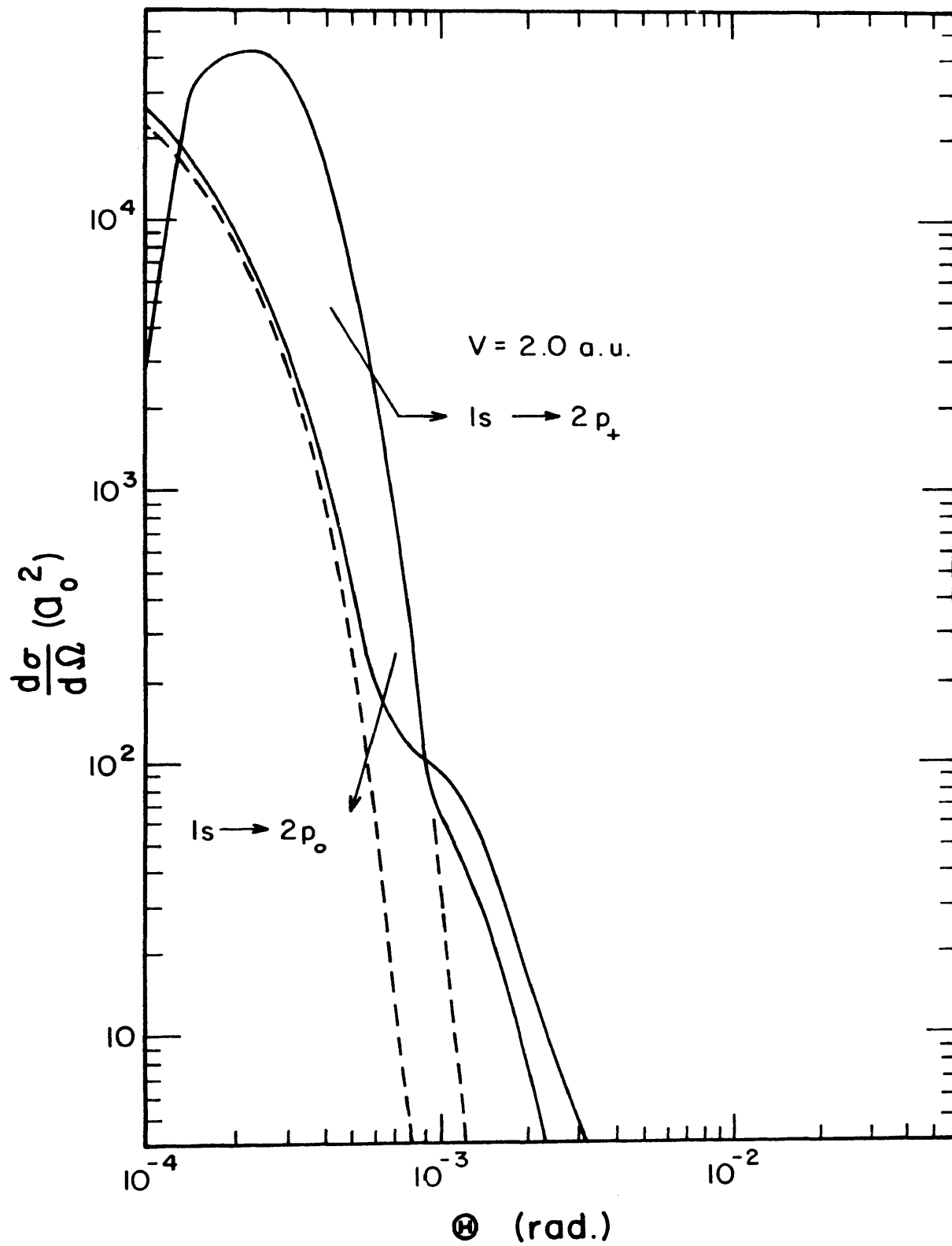
Figure 21

apply to these results.

2. Total Cross Sections

The total cross section for the 1s→2s excitation is presented in Fig. 22. The eikonal DWBA is compared to the first Born approximation and to the 4-state impact parameter calculation of Flannery[8] or Levy[9]. The experimental data are from the experiments of Orbeli, et al.[3,4], Birely and McNeal[10], and Hughes and Choe[11].

Likewise in Fig. 23, the total cross section is presented for the 1s→2p excitation. The source of the experimental data is the same as in the 1s→2s excitation with the addition of the experimental data of Dose, Gunz, and Meyer[5].

The eikonal DWBA results in Figs. 22 and 23 follow closely to the 4-state impact parameter results. This was expected from the analysis of the H-H scattering in section IV. The first Born approximation seems to predict the experimental data better than the other theoretical methods. However, since the validity of the first Born approximation is questionable at lower velocities, Levy[9] has pointed out that the agreement may be accidental.

The experimental data are from experiments that use the same general technique. That is, the cross sections are calculated from the intensity of the light emitted from the excited states of the hydrogen atoms. The Lyman-α radiation is emitted spontaneously from the H(2p) state and the intensity of the radiation gives a relative value for the population of the atoms that were in the 2p states.

FIG. 22. The total cross section for the excitation of hydrogen to the 2s state by helium impact. The solid line is the eikonal DWBA and the dashed line is the first Born approximation. The dash-dot line is the 4-state impact parameter calculation of Flannery, Ref. 8, or Levy, Ref. 9. The triangles represent the experimental data of Orbeli, et al., Refs. 3 and 4; the squares, Birely and McNeal, Ref. 10; and the circle-line, Hughes and Choe, Ref. 11.

Figure 22

FIG. 23.   The total cross section for the excitation of hydrogen

to the 2p states by helium impact.   The solid line is the eikonal DWBA

and the dashed line is the first Born approximation.   The dash-dot

line is the 4-state impact parameter calculation of Flannery, Ref. 8,

or Levy, Ref. 9.   The triangles represent the experimental data of

Orbeli, et al., Refs. 3 and 4; the squares, Birely and McNeal, Ref.
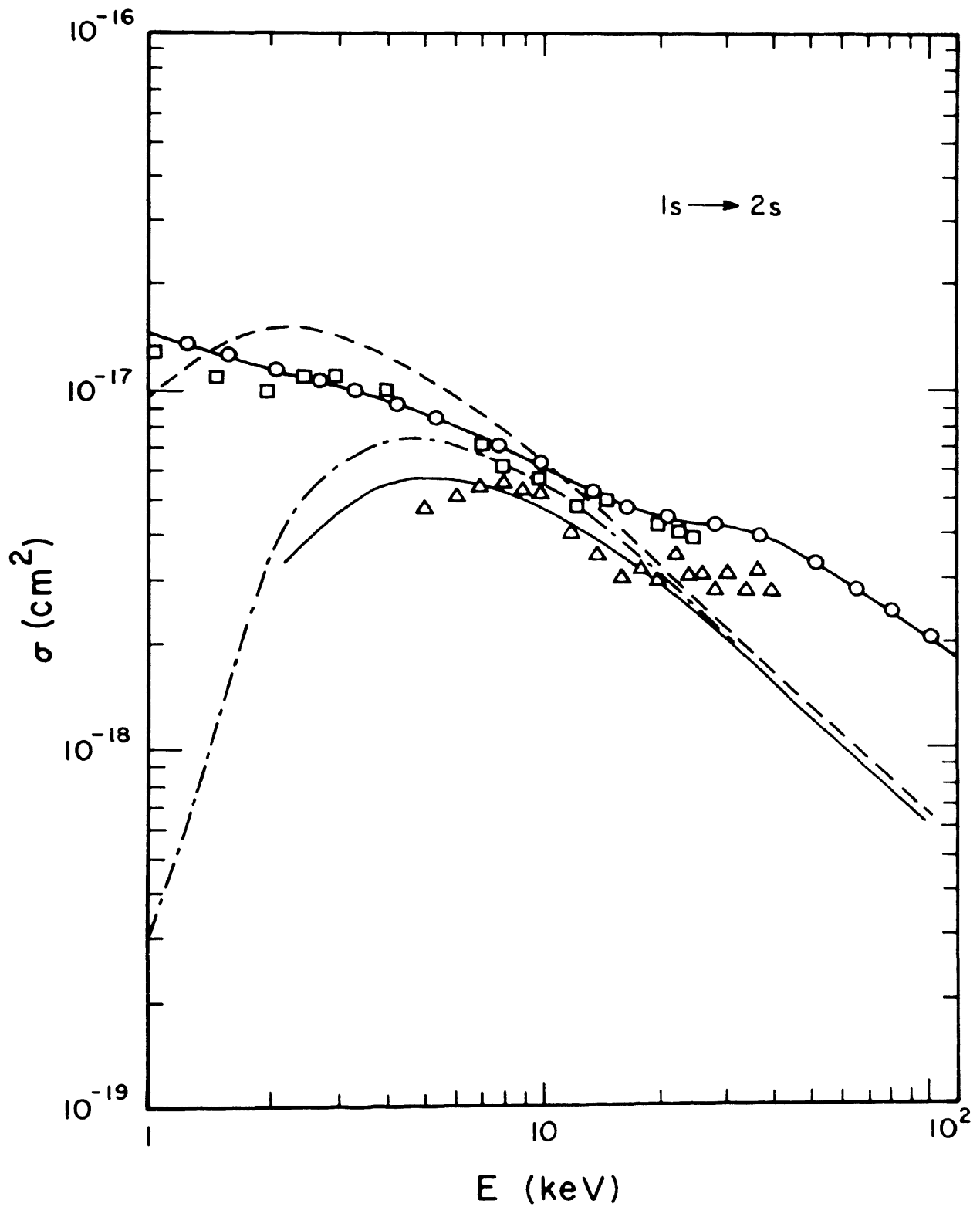
10; the hexagons, Dose et al., Ref. 5; and the circle-line, Hughes

and Choe, Ref. 11.
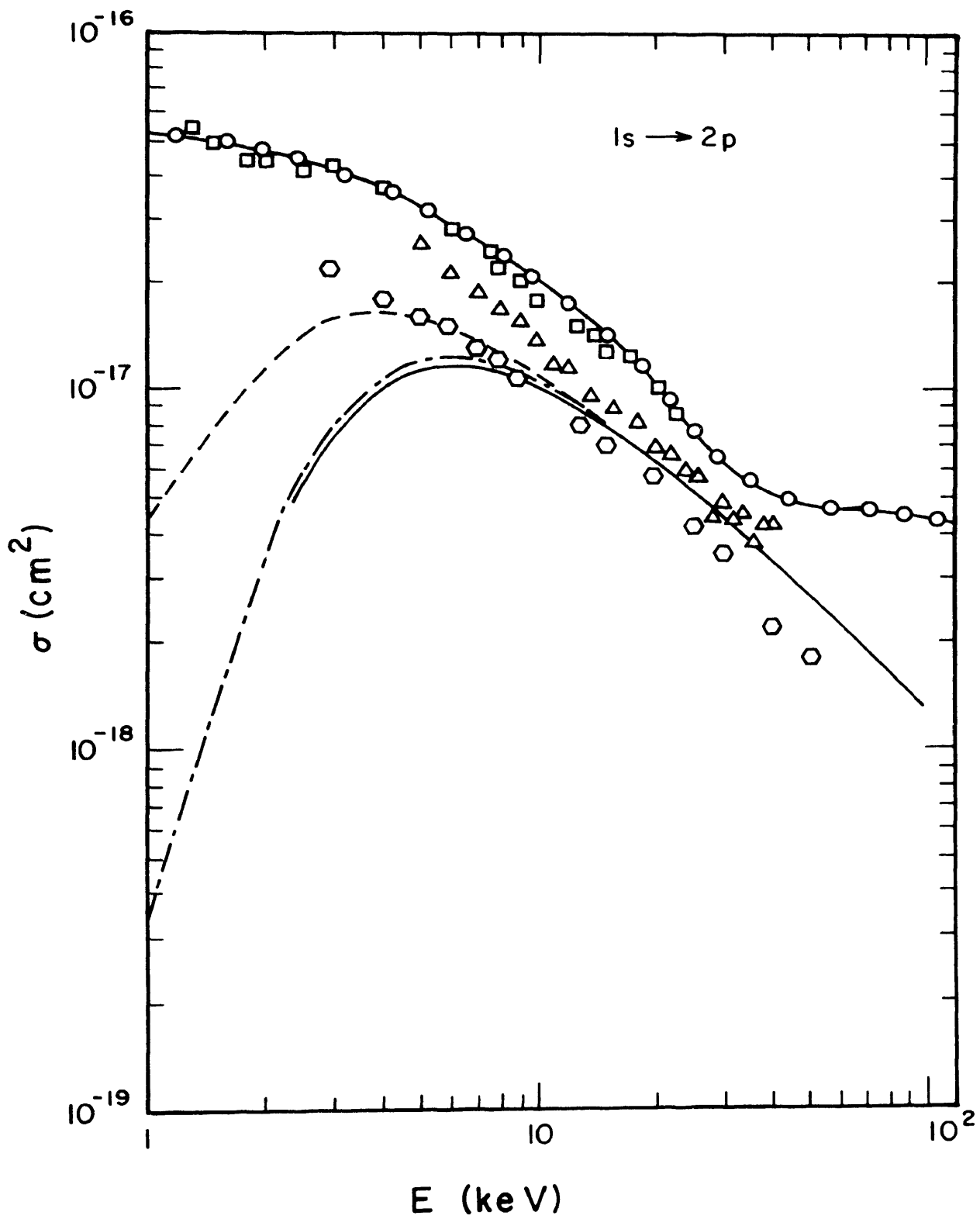
Figure 23

The addition of an electric field quenches the excited H(2s) atom and the resulting Lyman-α radiation can be used to find the relative population of the 2s state. Cascade effects into the 2s and 2p states could be important in the measurement of these cross sections. However, Birely and McNeal[10] and Hughes and Choe[11] have estimated the cascade effect to be small, 3-6 % for H(2s) and 10-15 % for H(2p). The more recent experiments of Birely and McNeal[10] and Hughes and Choe[11] have made several adjustments to improve their results over the earlier experiments of Orbeli, et al.[3,4], and Dose, et al.[5], and should be considered to be the more accurate experiments.

The region of the largest disagreement between the experimental data and the eikonal DWBA results is at low energy where the eikonal DWBA is not expected to be valid. At the lower energies electron exchange may become important. The question of electron exchange will be discussed in the next section.

VI. CONCLUSION

The eikonal DWBA presented here is at the moment the only means other than the first Born approximation to predict differential cross sections in the intermediate energy range for atom-atom collisions. As was seen in section V, the eikonal DWBA gave differential cross sections which compared quite favorably with the experimental data of Sauers, Nichols and Thomas[12]. However, the comparison of the total cross sections to the experimental data was in poor agreement at low energies.

The neglect of electron exchange can be a source of error in the calculation. There is some question at the moment as to the importance of electron exchange in the intermediate energy range. At low energies, it is obviously important since electron exchange is essential in the evaluation of molecular states.[39] At high energies, electron exchange is not considered since the electrons can be associated with one center or the other and the collision occurs in such a short time that the time needed for electrons to arrange themselves into molecular states is not available. The intermediate energy range could be said to possess characteristics of both energy extremes.

Consider electron exchange for the H-H collision. Even though the equations including electron exchange can be written down, the solution to the equations is difficult. The exchange term will contain a two-center integral that is similar to integrals that occur in the Heitler-London method[40] for the hydrogen molecule.

The two-center integral can be done in closed form for the hydrogen molecule in the ground state, but Slater[40] has pointed out that the exchange term for excited states cannot usually be done in closed form and that the evaluation of the exchange term must be performed numerically. Thus, the inclusion of electron exchange in the present calculation would be a formidable task and would greatly increase the computation time needed. The inclusion of exchange for systems with more electrons, such as the H-He collision, becomes increasingly more complicated.

The information for a particular collision channel is contained in the optical potentials and the off diagonal matrix elements. If the optical potentials and the off diagonal matrix elements can be found by some approximate means, then the eikonal DWBA can be used. One possibility is the use of generalized oscillator strengths. Levy[41] has used experimental generalized oscillator strengths to calculate the matrix elements for the excitation of H by Ne, Ar, and Kr, using the multistate impact parameter method. Also the Hartree-Fock potential of a complicated atom can be used in the calculation of the matrix elements. Flannery[8] started with the Hartree-Fock potential for He instead of the He wave function in his calculation for the H-He collision.

In the final analysis, I can conclude that the eikonal DWBA is a very promising approach to finding differential cross sections. Comparison to the experimental data shows relative agreement with the calculated differential cross sections. The total cross section of the eikonal DWBA was shown to reduce to the 2-state distortion

approximation in the limit of very small scattering angle and high energy. A comparison of the calculated total cross section to experimental data shows a strong disagreement at lower velocities.

VII. APPENDIX, NUMERICAL PROCEDURE

The numerical procedure used to solve the two dimensional integral for the T matrices (Eqs. (4.12)-(4.20)) was a standard Gaussian quadrature. Since this numerical procedure is so common, a listing of it is unnecessary. I will, however, mention a few specific peculiarities that may be of interest.

The infinite integration were performed as a sum of integrals over a small step size. When the sum converged to a particular value, the integration was stopped. However, since the integration was for an oscillating function, the convergence of the integral was not checked until the oscillation had died down. Since the off diagonal potential matrix elements (Eqs. (4.8)-(4.11)) are not long range and die off exponentially, the oscillations die out rapidly and the b and Z integrations did not have to be carried out very many steps to ensure convergence.

The oscillations of the Z integration were not very rapid, even for large scattering angles, so a larger step size could be chosen for it. The oscillation of the b integration was very rapid for small b, so a small step size was taken. For larger b, the step size could be larger, since the oscillations were not as rapid.

The integral for $\gamma(b,Z)$ was performed in a similar manner. At the end of each step of Z and b, the value of $\gamma(b,Z)$ was stored in a matrix. This was done since these values would be needed when the integral would be repeated for a different scattering angle. The value of $\phi(b)$ was then the value of $\gamma(b,Z)$ where Z was taken to be the largest value of Z that was stored in the matrix. This procedure

reduced the computation time by a factor of three and enabled the program to run in a reasonable amount of time.

The integration of the differential cross section over the solid angle $d\Omega$ gave the total cross section. The same numerical procedure was used. The step size was chosen small for small angles since the differential sections peak sharply for small angles. For larger angles the step size could be larger since the differential cross sections die off slowly with larger angles.

The program was checked by reproducing the values of the differential cross sections for e-H excitation given by Chen, Joachain, and Watson[14]. The step sizes for the b and Z integration were also varied and the step sizes, that were the largest, but yet gave the most accurate results, were used.

The program was written in Fortran V and run on an IBM 360, model 50. The time for the program to calculate the differential cross sections and the total cross section for a particular velocity was 30-60 minutes depending upon the number of points chosen to integrate the differential cross section. The total time to generate all the results presented in the H-H and H-He sections was over 25 hours.

VIII. BIBLIOGRAPHY

1. D. R. Bates and G. W. Griffing, Proc. Phy. Soc. A $\underline{66}$, 961 (1953).

2. B. L. Moisewitsch and A. L. Stewart, Proc. Phys. Soc. A $\underline{67}$, 1069 (1954).

3. V. A. Ankudinov, E. P. Andreev, and A. L. Orbeli, in Proceedings of the Fifth International Conference on the Physics of Electronic and Atomic Collision, edited by I. P. Flaks (publishing House "Nauka", Leningrad, USSR, 1967), p. 312.

4. A. L. Orbeli, E. P. Andreev, V. A. Ankudinov, and V. M. Dukelskii, Zh. Eksp. Teor. Fiz $\underline{57}$, 108 (1969) [Sov. Phy. JETP $\underline{30}$, 63 (1970)].

5. V. Dose, R. Gunz, and V. Meyer, Helv. Phys. Acta $\underline{41}$, 264 (1968).

6. M. R. Flannery, Phys. Rev. $\underline{183}$, 231 and 241 (1969).

7. Projectiles with velocities much less than 2×10^8 cm/sec (velocity of an average outer electron) are considered low energy. High and intermediate energies are then defined in a consistent manner.

8. M. R. Flannery, J. Phys. B $\underline{2}$, 913 (1969).

9. H. Levy II, Phys. Rev. $\underline{187}$, 136 (1969).

10. J. H. Birely and R. J. McNeal, Phys. Rev. A $\underline{5}$, 257 (1972).

11. R. H. Hughes and Song-Sik Choe, Phys. Rev. A $\underline{5}$, 1758 (1972).

12. I. Sauers, T. W. Nichols, and E. W. Thomas, Bull. Am. Phys. Soc. $\underline{17}$, 1130 (1972).

13. R. J. McNeal and J. H. Birely, "Laboratory Studies of Collisions of Energetic H^+ and H with Atmospheric Constituents", in press to Review of Geophysics and Space Physics.

14. J. C. Y. Chen, C. J. Joachain, and K. M. Watson, Phys. Rev. A 5, 2460 (1972).

15. N. F. Mott and H. S. W. Massey, The Theory of Atomic Collisions (Clarendon Press, Oxford, England, 1965), 3rd ed., p. 428.

16. D. R. Bates, Atomic and Molecular Processes (Academic Press, New York, 1962), p. 597.

17. S. Geltman, Topics in Atomic Collision Theory (Academic Press, New York, 1969), p. 175.

18. M. R. C. McDowell and J. P. Coleman, Introduction to the Theory of Ion-Atom Collisions (North-Holland / American Elsevier, New York, 1970), p. 171.

19. Atomic units (a.u.) will be used throughout this thesis. Distances are in Bohr radii (a_0 = .529 $\times$ 10^{-8} cm). Charge and Mass will be measured in terms of the electron charge and mass (e = 1.6 $\times$ 10^{-19} C and m = 9.11 $\times$ 10^{-28} gm). One atomic unit of velocity, energy, and cross sections are 2.19 $\times$ 10^{8} cm/sec, 27.2 eV, and .28 $\times$ 10^{-16} cm^2, respectively.

20. Ref. 15, p. 86; Ref. 16, p. 550; Ref. 17, p. 103; and Ref. 18, p. 310.

21. Ref. 16, p. 578; Ref. 17, p. 192; and Ref. 18, p. 108.

22. R. J. Glauber, in Lectures in Theoretical Physics, edited by W. E. Brittin, et al. (Interscience, New York, 1959), Vol. I, p. 315.

23. V. Franco, Phys. Rev. Lett. 20, 709 (1968).

24. K. Bhadra, and A. Ghosh, Phys. Rev. Lett. 26, 737 (1971).

25. H. Tai, R. H. Bassel, E. Gerjuoy, and V. Franco, Phys. Rev. A 1, 1819 (1970).

26. V. Franco, Phys. Rev. A 1, 1705 (1970).

27. A. C. Yates and A. Tenney, Phys. Rev. A 6, 1451 (1972).

28. F. W. Byron, Jr., Phys. Rev. A 4, 1907 (1971).

29. V. Franco, Phys. Rev. Lett. 26, 1088 (1971).

30. Ref. 17, p. 230.

31. M. L. Goldberger and K. M. Watson, Collision Theory (John Wiley & Sons, New York, 1964), p. 202.

32. A. L. Fetter and K. M. Watson, Advances in Theoretical Physics, edited by K. A. Brueckner (Academic Press, New York, 1965), Vol. I, p. 115.

33. C. Bottcher and M. R. Flannery, J. Phys. B 3, 1600 (1970).

34. B. Ritchie, Phys. Rev. A 3, 656 (1971).

35. Ref. 17, p. 196 and Ref. 18, p. 123.

36. Ref. 17, p. 205.

37. B. Ritchie, Phys. Rev. A 2, 759 (1970).

38. F. W. Byron, Jr., and C. J. Joachain, Phys. Rev. 146, 1 (1966).

39. J. C. Slater, Quantum Theory of Molecules and Solids (McGraw-Hill, New York, 1963), Vol. I, p. 41.

40. Ref. 39, p. 263.

41. H. Levy, II, Phys. Rev. A 1, 750 (1970).

IX. VITA

Richard Homer Shields was born on June 5, 1945, in Paris, Illinois. He received his primary and secondary education in Mattoon, Illinois. He has received a Bachelor of Science in Education in 1967 and a Master of Science in 1969 from Eastern Illinois University.

He has been enrolled in the Graduate School of the University of Missouri-Rolla since September, 1969, and has held a National Defense Education Act fellowship for the period of September 1969 to August 1972 and a teaching assistantship from September 1972 to May 1973.

He is married to the former Barbara Simpson of Loami, Illinois.